Chemosphere 211 (2018) 50–61

Contents lists available at ScienceDirect

Chemosphere

journal homepage: www.elsevier.com/locate/chemosphere

Bioavailability and preservation of organic phosphorus in lake sediments: Insights from enzymatic hydrolysis and ^{31}P nuclear magnetic resonance

Yuanrong Zhu [a], Weiying Feng [a], Shasha Liu [a], Zhongqi He [b], Xiaoli Zhao [a, *], Yong Liu [c, d], Jianyang Guo [d], John P. Giesy [a, e], Fengchang Wu [a]

[a] State Key Laboratory of Environment Criteria and Risk Assessment, Chinese Research Academy of Environmental Sciences, Beijing 100012, China
[b] USDA-ARS Southern Regional Research Center, 1100 Robert E Lee Blvd, New Orleans, LA 70124, USA
[c] School of Biological and Environmental Engineering, Guiyang University, Guiyang, 550005, China
[d] State Key Laboratory of Environmental Geochemistry, Institute of Geochemistry, Chinese Academy of Sciences, Guiyang 550002, China
[e] Department of Biomedical and Veterinary Biosciences and Toxicology Centre, University of Saskatchewan, Saskatoon, Saskatchewan, Canada

HIGHLIGHTS

- P_o was extracted by NaOH-EDTA, which few remained in the residual sediments.
- P_o was characterized by a combination of enzymatic hydrolysis and ^{31}P NMR.
- 54.6–100% of P_o measured by ^{31}P NMR could be hydrolyzed by the phosphatase.
- Labile P_o in sediments was an important source of bioavailable P for algal blooming.
- Bioavailability and preservation of P_o was influenced by organic matter and minerals.

GRAPHICAL ABSTRACT

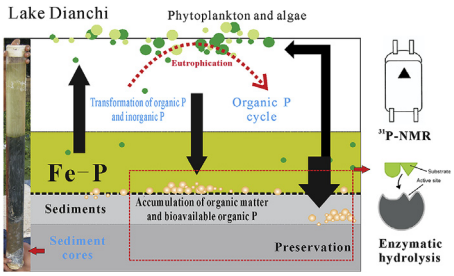

ARTICLE INFO

Article history:
Received 14 May 2018
Received in revised form
14 July 2018
Accepted 22 July 2018
Available online 24 July 2018

Handling Editor: X. Cao

Keywords:
Organic phosphorus
Enzymatic hydrolysis
^{31}P NMR
Bioavailability
Preservation
Sediments

ABSTRACT

Bioavailability and preservation of organic P (P_o) in the sediment profiles (DC-1 and DC-2) from Lake Dianchi, a eutrophic lake in China, were investigated by a combination of enzymatic hydrolysis and solution ^{31}P nuclear magnetic resonance (NMR) spectroscopy. Results showed that large of P_o could be extracted by NaOH-EDTA (NaOH-EDTA P_o), with little P_o in residues after extraction with NaOH-EDTA. Bioavailability and preservation of NaOH-EDTA P_o provide key information for biogeochemical cycling of P_o in sediments. The details of P species and their bioavailability in NaOH-EDTA P_o showed that 54.8–70.4% in DC-1 and 54.6–100% in DC-2, measured by ^{31}P NMR, could be hydrolyzed by the phosphatase. Whereas, some proportion of NaOH-EDTA P_o could not be hydrolyzed by the phosphatase, and decreased with sediment depth. Interaction between P_o and other organic matter (e.g., humic acids) is likely an important factor for preservation of these P_o in the sediment profiles. Simulation experiments of hydrolysis of model P_o compounds adsorbed by minerals, such as goethite and montmorillonite, further indicated that adsorption to minerals protected some P_o, especially phytate-like P, from enzymatic hydrolysis, thus preserving these forms of P_o in sediments. Interactions of P_o with organic matter and minerals in the sediments are two important factors determining biogeochemical cycling of P_o in lakes.

* Corresponding author.
E-mail address: zhaoxiaoli_zxl@126.com (X. Zhao).

https://doi.org/10.1016/j.chemosphere.2018.07.134

Intervention to break the cycle of Fe–P and bioavailable P_o (e.g., labile monoester P) in the history of eutrophication is important way to control algal blooming.

1. Introduction

Eutrophication is a primary water quality issue for freshwaters of the world (Carpenter et al., 1999; Smith and Schindler, 2009). Phosphorus (P) is an essential nutrient and is one of the key factors limiting primary production in lake ecosystems, and a determinant of eutrophication (Schindler, 1977; Conley et al., 2009; Ding et al., 2018). Once external P inputs are controlled, internal P recycling is the most important supply of P for primary production and maintaining the trophic status and algal blooming (Zhu et al., 2013b, 2013c; Chen et al., 2018). Organic P (P_o), which can constitute a substantial pool of internal P from lake sediments, has received much more attention as the development and application of multiple analytic methods in recent years (Worsfold et al., 2008; Zhu et al., 2013b; Giles et al., 2015). Especially, bioavailable P_o forms in sediments and their biogeochemical cycling are important mechanisms to self-regulate P status in lakes and maintain their eutrophic status (Zhu et al., 2013b; Giles et al., 2015). Instead, preservation of P in sediments is an important way to reduce active P levels in lakes. For examples, addition of aluminum (Al) dosing has been used in lakes worldwide (Jensen et al., 2015), to preserve P, including some P_o in the sediments (Reitzel et al., 2006). Thus, it is important to understand mechanisms affecting bioavailability and preservation of P_o, and even its relationships between internal cycling of P_o and trophic status of lakes.

Solution ^{31}P nuclear magnetic resonance (NMR) spectroscopy and enzymatic hydrolysis have been used separately or in combination, to characterize forms and bioavailability of P_o in sediments (Zhu et al., 2013b, 2015b; Giles et al., 2015). ^{31}P NMR spectroscopy, which distinguishes specific P compounds and classes (e.g., orthophosphate monoester, diester, phosphonates and polyphosphate) in alkaline extracts of sediments, has advanced our knowledge of P_o in sediments more than any other technique (Ahlgren et al., 2005; Zhang et al., 2008; Ding et al., 2013; Giles et al., 2015). Most of these P_o are hydrolyzed to release phosphate prior to uptake by algae or other organisms (Herbes et al., 1975; Bünemann, 2008). Enzymatic hydrolysis, as a biotic method, plays a key role in liberation of phosphate from these P_o compounds satisfying the need of P for growth of plants, including algae (Herbes et al., 1975). Thus, enzymatic hydrolysis can provide an estimate of bioavailable P_o, such as labile monoester P, diester, and phytate-like P (He and Honeycutt, 2001; Monbet et al., 2007; Zhu et al., 2013b).

A combination of enzymatic hydrolysis and ^{31}P NMR provides not only complementary information on P species and their bioavailability (Giles et al., 2015), but also information on preservation of P_o in sediments (Zhu et al., 2015b). Based on results of previous studies that have combined these techniques (Zhu et al., 2015b), natural organic matter, such as humic acid, can be a significant factor determining bioavailability and preservation of some P_o such as phytate-like P in the surficial sediments. Additionally, minerals, such as Fe or Al oxides, were the main composition of lake sediments, which would adsorb a range of P_o (Ruttenberg and Sulak, 2011). Importantly, research has suggested that preservation of P_o would be enhanced by increasing immobilization by adsorption to solids in sediment profiles (Ding et al., 2013). Minerals have been shown to protect adsorbed inositol hexakisphosphate (IHP) from enzymatic hydrolysis (Giaveno et al., 2010), which indicated that preservation of IHP would be enhanced when adsorption by minerals surfaces. Whereas, surface of some minerals, such as goethite, would be effective in concentrating substrates and enzymes, where enzymatic hydrolysis of some labile monoester P_o (e.g., gucose-1-phosphate) also can be of the same order of magnitude as in aqueous solution (Olsson et al., 2011). Therefore, investigation of influence of minerals on bioavailability and preservation of P_o would be important for further understanding biogeochemical cycling of P_o in sediments of lakes.

However, little information about bioavailability and preservation of P_o from sediment, especially sediment profiles is available (Giles et al., 2015). In this study, bioavailability and preservation of P_o in the sediment profiles from Lake Dianchi were analyzed by enzymatic hydrolysis and ^{31}P NMR. The influence of organic matter on bioavailability and preservation of P_o was further investigated in the sediment profiles based on previous studies (Zhu et al., 2015b). Especially, the influence of minerals (goethite and montmorillonite) on the bioavailability and preservation of P_o was also investigated in this study. Finally, biogeochemical cycling of P_o and its relationship with eutrophication of Lake Dianchi are discussed.

2. Materials and methods

2.1. Study site and sample collection

Lake Dianchi (24°40′–25°02′ N, 102°36′–102°47′ E) is a shallow, eutrophic lake located in the city of Kunming, Yunnan Province, Southwest China (Fig. S1, Supplementary data). It has an area of approximately 306 km^2, with an average depth of approximately 5 m. Due to loading of contaminants and nutrients from industry and agriculture in recent decades, the lake is now severely eutrophic (Wang et al., 2009; Xiong et al., 2010). With good enforcement capacity, nutrients inputs have been reduced in recent years (Lu et al., 2012). However, quality of surface water has not improved markedly. There are still undesirable harmful algal blooms in water bodies every year. Internal cycling of nutrients is a major factor that continues to influence the trophic status of the lake (Gao et al., 2005; Zhu et al., 2013b). Lake Dianchi is a relatively closed system with a residence period of water from 3 to 8 years, which might exacerbate retention and accumulation of nutrients in the lake.

Due to both nutrients and wind conditions, algal blooms aggregate in north of Lake Dianchi. Additionally, organic matter and nutrients also accumulated in the sediments of center of Lake Dianchi (Zhu et al., 2013b). Thus, typical sediment cores at the site of DC-1 (24°56′27.48″ N, 102°39′50.51″ E) and DC-2 (24°50′36.24″ N, 102°42′54.49″ E) were collected in April 2010 from the north and the center of Lake Dianchi (Fig. S1) by use of a homemade piston-percussion corer (Reasoner, 1993) fitted with 5-cm internal plexiglass cylindrical tubes.

Sediments were sectioned into 1-cm intervals (in the top 20 cm) and 3-cm intervals (below 20 cm) immediately after collection, and then lyophilized. Samples were ground to powder with a pestle and mortar, and were stored in the freezer at temperature between 0 and −20 °C until analysis.

2.2. Chemical analysis

Total contents of Al, Ca, Fe and Mn in sediments were measured by use of an inductively coupled plasma-optical emission spectroscopy (Perkin-Elmer Optima 5300 DV, USA) after microwave-acid wet digestion by HNO_3, HCl, and HF (Sneddon et al., 2006). Subsamples of sediments were pretreated with 1 M HCl to remove carbonates, and then total organic carbon (TOC) and total nitrogen (TN) were analyzed by using an elemental analyzer (Vario EL III, Elementar, Germany). Carbon and nitrogen isotope analyses were conducted on a Delta ^{plus} XP mass spectrometer connected with a Flash EA elemental analyzer (Thermo Finnigan, Germany). $\delta^{13}C$ and $\delta^{15}N$ are reported as per mil relative to Vienna Pee Dee Belemnite and air, respectively.

Basic composition of P in sediments was determined by use of the Standards, Measurements and Testing (SMT) protocol of the European Commission (Ruban et al., 1999, 2001). The operationally defined scheme was composed of five steps: NaOH soluble inorganic P (Fe/Al–P, P bound to Al, Fe and Mn oxides and hydroxides), HCl extractable inorganic P (Ca–P, P associated with Ca), organic P (P_o), inorganic P (P_i), and total P (TP). For each P fraction, the concentrations were determined by use of the molybdenum blue method (Murphy and Riley, 1962).

2.3. Organic P extraction

Sediment (1.0 g) was first treated with 30 mL of 0.1 M HCl by shaking for 1 h at room temperature to remove cations that could interfere with subsequent extraction of P_o (Turner et al., 2005). It is also important to obtain a relatively large ratio of P_o to P_i (removing some proportion of P_i, such as calcium bounded P_i) for enzymatic hydrolysis. After centrifugation (10000 g, 15 min) the supernatant was decanted. Sediment was then extracted by shaking with 30 mL of a solution containing 0.25 M NaOH and 50 mM Na_2EDTA for 16 h at room temperature (Turner and Weckström, 2009; Zhang et al., 2009; Ding et al., 2010). NaOH-EDTA extracts were centrifuged at 10000 g for 30 min. Inorganic P in diluted extracts was determined by the molybdenum blue/ascorbic acid method (Murphy and Riley, 1962). Total P in extracts was determined after $K_2S_2O_8$ digestion. The P_o content in the NaOH-EDTA extracts (NaOH-EDTA P_o) was calculated as the difference between TP and P_i. The remaining extracts were stored at −20 °C until enzymatic hydrolysis and ^{31}P NMR analysis.

In order to examine P_o in sediment residues after extraction by NaOH-EDTA, selected residues after NaOH-EDTA extraction were further sequentially extracted by a detailed P_o scheme of Golterman (1996); Golterman et al. (1998), and then analyzed by solution ^{31}P NMR again (Fig. S2). Each sediment-suspension was centrifuged (10000 g) for 15 min, decanted, and an aliquot was taken for quantification of P. To determine the P in the extracts such as Ca- and Na-EDTA, a 25–50 time dilution was done to prevent the interferences of chelating reagents with the Mo–P colorimetric reaction. The P_o in the fractions was quantified by $K_2S_2O_8$ digestion. The remaining water, CaEDTA, NaEDTA, H_2SO_4 (neutralization by NaOH), cold TCA [trichloroacetic acid] (0 °C), hot TCA (95 °C) and NaOH extracts were mixed and this fraction was defined as extractable residual P (ERP). Mixtures were lyophilized and stored at −20 °C until redissolution and analysis.

2.4. Enzymatic hydrolysis

Alkaline phosphatase (APase), phosphodiesterase (PDEase), and crude phytase from wheat were purchased from Sigma (P7640, P4506 and P1259). Details of the procedure for enzymatic hydrolysis have been described previously (Zhu et al., 2013b, 2015b). Briefly, stock enzyme solutions of APase (2 unit mL^{-1}) or PDEase (0.02 unit mL^{-1}) were prepared in Tris-HCl buffer (0.1 M, pH 9.0). Purified phytase was prepared in either a Tris-HCl buffer (0.1 M, pH 7.0) or a NaAc buffer (0.1 M, pH 5.15) at a concentration of 0.06 unit mL^{-1}. Exactly 0.3 mL of NaOH-EDTA extracts were neutralized, diluted, buffered and added 0.44 mL prepared enzyme solutions (pH 9.0 for APase, PDEase combined with APase; and pH 7.0 for APase, PDEase and phytase mixture) to make a final volume of 8 mL in a 10-mL tube. Enzymatic hydrolysis of P_o in these solutions was performed by incubating at 37 °C for 16 h. Blank NaOH-EDTA extracts in the absence of enzyme, and calibration P standards in the presence of both the extracts dilution and enzyme solutions were also incubated simultaneously as controls. Inorganic P released was quantified by molybdenum blue method (Murphy and Riley, 1962). Each extract was analyzed in triplicate and the mean calculated.

Based on this procedure and substrate specificity tests of these enzymes (Zhu et al., 2013b), three classes of enzymatically hydrolyzable P were quantified as: (1) labile monoester P and condensed P (hydrolyzed by APase); (2) diester P (hydrolyzed by the mixture of APase and PDEase minus labile monoester P and condensed P); (3) phytate-like P (hydrolyzed by the mixture of APase, PDEase and phytase minus diester P and labile monoester P and condensed P). Additionally, the portion of P_o that was not hydrolyzed by APase, PDEase and phytase would be "unidentified P_o".

2.5. Solution ^{31}P NMR analysis

Lyophilized NaOH-EDTA extracts were redissolved in 2 mL D_2O, and shaken by ultrasonic vibration. Excess Na_2S (dissolved in D_2O) was then added to precipitate paramagnetic ions (e.g., Fe and Mn) and maintain reducing conditions (Vestergren et al., 2012). For some samples, MDPA (methylene diphosphonic acid sodium salt, 20 μL of 25 mM solution in D_2O, Sigma-Aldrich) was added as an internal standard. After setting aside for 17–20 h at 4 °C, each sample was centrifuged (10000 g, 30 min) and the supernatant was transferred to a 5 mm diameter NMR tube. The lyophilized ERP extracts were also redissolved by 1 M NaOH/D_2O and pretreated according to the NaOH-EDTA extracts.

Solution ^{31}P NMR spectra were recorded at 298 K using Agilent DD2 500 or 600 spectrometer (Agilent technologies), equipped with a 5 mm OneNMR probe. Spectra were collected with parameters setting as a 45° pulse (5.3 μs pulse duration), an acquisition time of 0.6 s, a relaxation delay of 5 s, and 12000–15000 scans. Peak areas were calculated by integration on spectra processed with 2 Hz line broadening, using a commercial NMR software package (MestRenova 9.0). Concentration of each P species was calculated by multiplying its relative contribution to total NMR signal by the total NaOH-EDTA extractable P concentration as determined above. A dilute P standards spike (dissolved in NaOH-EDTA extracts from sediments directly) was used to confirm the chemical shifts. Peak assignments were based on the spiking experiments and relative chemical shifts referred to previous reports (Cade-Menun, 2015; Giles et al., 2015).

2.6. Enzymatic hydrolysis of model P compounds adsorbed by minerals

In order to investigate influence of minerals on the bioavailability and preservation of P_o, a simulation experiment was designed. Five model P compounds representing a variety of molecular sizes and functional types were purchased from Sigma-Aldrich Chemicals (Shanghai, China). They were labile monoester

phosphate (glucose-6-phosphate, G6P; adenosine 5′ monophosphate, AMP; *p*-nitrophenyl phosphate, *p*NPP), phytate (inositol hexakisphosphate, IHP), and condensed-P compounds (pyrophosphate, Pyr). Solutions of G6P, AMP, *p*NPP, and Pyr containing 500 μM P were prepared by dissolution in 0.01 M Tris-HCl buffer (pH 9.0). Solution of IHP containing 1800 μM P was prepared by dissolution in 0.02 M NaAc-HAc buffer (pH 5.15). The final concentrations of P in these prepared solutions were further determined after digestion.

Goethite was one of the main authigenic mineral in sediment of Lake Dianchi (Zhang et al., 1996), montmorillonite was also an important clay mineral in sediments of Lake Dianchi (Xiao et al., 2012). Thus, goethite and montmorillonite were selected as two representative minerals from sediments of Lake Dianchi. Goethite was prepared by the method of Atkinson et al. (1967). The synthetic goethite was confirmed by powder X-ray diffraction analysis (Bruker D8 Advance, Germany) (Fig. S3). Montmorillonite KSF purchased from Alfa Aesar (A Johnson Matthey Company).

Based on results from previous studies of adsorption and desorption of P_o onto minerals (Ruttenberg and Sulak, 2011; Johnson et al., 2012), pre-sorbed samples of P (Minerals-P complexes) were prepared. Briefly, 200 mg minerals were weighed into 50 mL polypropylene tubes, to which 30 mL of prepared P solution was added then shaking for 17 h at 25 °C. The tubes were centrifuged, and aliquots of supernatant collected for quantification of P, while the remainder was discarded. Particles (Minerals-P complexes) were lyophilized and prepared for enzymatic hydrolysis.

Aliquots of 20 mg minerals-P_o complexes containing G6P, AMP, *p*NPP were weighed into 50 mL polypropylene tubes respectively, and then 10 mL APase buffer solutions (0.01 M Tris-HCl, pH 9.0) were added. Suspensions were incubated at 25 °C for 1 h. Minerals-P_o complexes in the absence of enzymes were controls for any non-enzymatic hydrolysis of P_o. Incubated suspensions were then centrifuged. Aliquots of supernatant were collected for P analysis. In order to check the hydrolysis of P_o in the P_o-mineral complexes, precipitated particles were extracted by 0.25 M NaOH solution for 16 h. After centrifugation, supernatant were collected for P analysis.

2.7. Statistical analysis

Statistical analysis was performed using v19.0 software. The correlations between each two variables were individually analyzed using the Pearson correlation coefficient, at the $p < 0.05$, $P < 0.01$ or $P < 0.001$ levels of significance.

3. Results

3.1. Bulk compositions of organic matter and selected metals in sediments

Based on vertical profiles of TOC, TN, TOC/TN (molar ratio), $\delta^{13}C$ and $\delta^{15}N$ (Fig. S4), the sediment profiles can be approximately categorized into two distinct stages in the evolution of Lake Dianchi. In the lower section (Section 1: 55–12 cm), the organic matter content was relatively constant, though the TOC, TN, and TOC/TN gradually increased in a downward direction below 40 cm. However, in the upper section (Section 2: 12–0 cm), TOC and TN increased markedly in both cores. There was an increase in accumulation of TOC from 2.5% to 9.6% in DC-1, and from 1.6% to 7.5% in DC-2. TN ranged from 0.3% to 1.1% in DC-1, and from 0.2% to 0.8% in DC-2. The TOC/TN ratio was relatively constant in DC-1, and varied from 8.6 to 11.7; the range in DC-2 was from 7.0 to 13.5. Bulk isotope compositions of sediments display positive shifts in $\delta^{13}C$ and $\delta^{15}N$ in this section.

Distribution of Al, Ca, Fe, and Mn contents were similar in sediment profiles from DC-1 and DC-2 (Fig. S5). Contents of Al and Ca decreased as the depth of sediment increased. However, contents of Fe increased with depth from 0 to 20 cm, and then decreased slowly below 20 cm. Contents of Mn were low, which were fluctuated through sediment cores from Lake Dianchi.

3.2. Basic composition of phosphorus in sediments

Vertical variations of P fractions in the two sections of sediment profiles (Fig. S6) were similar to those of bulk composition of organic matter. However, contents of TP, P_i, and its fractions increased as sediment depth increased from 0 to 4 cm, except for P_o. Contents of P fractions were greater in DC-2 than in DC-1. Inorganic P was divided into Fe/Al–P and Ca–P, which was the main component of TP in sediments from Lake Dianchi. Trends in P_o were different from trends in P_i in Section 1, and concentrations of P_o have continued to increase in recent years (0–4 cm sediments). Contents of P_o determined by SMT protocol varied from 290.6 to 492.1 mg kg^{-1} and from 357.3 to 663.7 mg kg^{-1} in DC-1 and DC-2, respectively, and accounted for 23.7–32.9% and 19.2%–34.8% of TP in sediments. Fractions of P in sediments from Lake Dianchi were in the order that Ca–P > P_o > Fe/Al–P.

3.3. NaOH-EDTA extractable P_o and the residual P

Contents of NaOH-EDTA P_o including condensed P ranged from 30.8 to 269.0 mg kg^{-1} and 30.1 to 220.0 mg kg^{-1}, and accounted for 2.1–12.5% and 1.6–9.3% of TP in sediments from DC-1 and DC-2, respectively (Fig. 1, Tables S1 and S2 in Supplementary data). Contents of NaOH-EDTA P_o decreased with sediment depth, and then stabilized gradually. Contents of NaOH-EDTA P_o were significantly correlated with TOC (%) in both sediment cores (DC-1: $r^2 = 0.98$, $p < 0.001$, $n = 24$; DC-2: $r^2 = 0.91$, $p < 0.001$, $n = 31$). However, there were only 7.2–43.8% and 5.4–35.8% respectively of total P_o determined by SMT protocol extracted by NaOH-EDTA in DC-1 and DC-2 sediments (Tables S1 and S2). Especially, the proportion of NaOH-EDTA P_o in TP or total P_o determined by SMT method decreased rapidly with sediment depth. Thus, residual P after extraction by NaOH-EDTA was further determined by sequential extraction combined with solution ^{31}P NMR analysis. Results of sequential extraction showed that little P_o was extracted by the other chelating solvents, such as H_2SO_4, TCA and hot NaOH (Table S3). However, there was no detectable P_o or condensed P identified by solution ^{31}P NMR spectroscopy of the extractable residual P (ERP) (Fig. S7). Additionally, only a small proportion of P remained after NaOH-EDTA extraction and sequential extraction by other chelating compounds (Table S3).

3.4. Enzymatic hydrolysis of NaOH-EDTA P in sediments

To estimate the bioavailability of NaOH-EDTA P_o in the sediment profiles, enzymatic hydrolysis of NaOH-EDTA P_o was quantitatively analyzed (Fig. 1, Tables S1 and S2). APase activities can hydrolyze labile monoester P and condensed P (Monbet et al., 2007; Zhu et al., 2013b). Contents of NaOH-EDTA P_o hydrolyzed by APase were 3.0–82.4 mg kg^{-1} and 6.5–100.3 mg kg^{-1} and accounted for 9.6–43.2% and 15.1–73.3% of NaOH-EDTA P_o in the DC-1 and DC-2 sediment profiles, respectively. PDEase combined with APase can hydrolyze labile monoester P, condensed P, and diester P. Therefore, more P_o was hydrolyzed to phosphate by a combination of PDEase and APase for NaOH-EDTA extracts than by APase alone. Concentrations of P_o released by PDEase and APase varied from 7.9 to 119.9 mg kg^{-1} in DC-1 and from 15.5 to 124.0 mg kg^{-1} in DC-2, and accounted for 25.6–72.5% and 34.1–100% of NaOH-EDTA P_o in DC-1

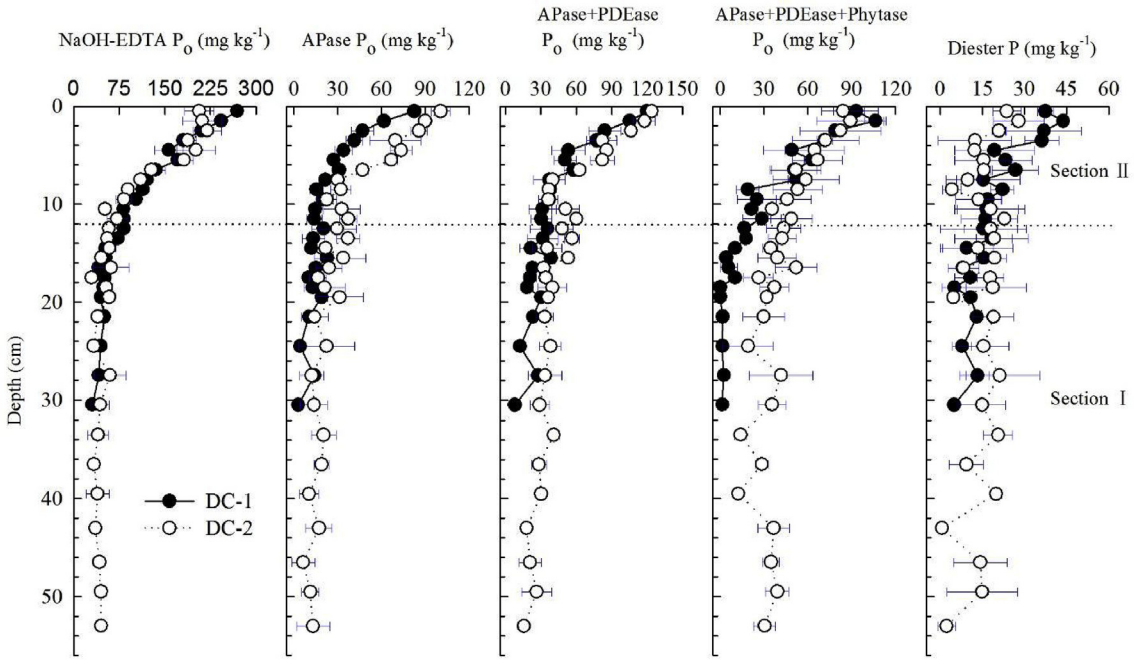

Fig. 1. Concentrations of NaOH-EDTA P_o and NaOH-EDTA P_o hydrolyzed by phosphatase in sediment profiles. APase P_o, NaOH-EDTA P_o hydrolyzed by APase (labile monoester P and condensed P); AP + PDE P_o, NaOH-EDTA P_o hydrolyzed by APase and PDEase; APase + PDEase + phytase P_o, NaOH-EDTA P_o hydrolyzed by APase, PDEase and phytase; Diester P, the difference between NaOH-EDTA P_o hydrolyzed by APase + PDEase and APase. Data are presented as the average value with standard deviation (n = 3).

and DC-2, respectively. Based on the difference between P_o hydrolyzed by APase alone and mixtures of PDEase and APase, the bioavailable diester P was also analyzed (Fig. 1). Phytase can hydrolyze a range of P compounds, including the inositol phosphates that cannot be hydrolyzed by PDEase and APase. However, the amount of P_o released from extracts by APase, PDEase, and phytase at pH 7 was not greater for most samples. Amounts of NaOH-EDTA P_o hydrolyzed by these phosphatases in DC-1 varied from 0 to 106.3 mg kg^{-1}, and accounted for 0–43.8% of NaOH-EDTA P_o; in DC-2, the amounts varied from 12.4 to 89.1 mg kg^{-1}, and accounted for 31.2–100.0% of NaOH-EDTA P_o. Bioavailability of P_o decreased with depth in the sediment profiles of the upper section (Section 2), and then became constant in sediment profiles of Section 1 (Fig. 1).

3.5. Solution ^{31}P NMR spectroscopy of NaOH-EDTA P in sediments

Solution ^{31}P NMR spectra of NaOH-EDTA extractable P could be found in Fig. S8. Based on results of spiking experiments and peak identification (Fig. 2), concentrations and percentage of P species of NaOH-EDTA P were given in Table 1. Ortho-P, the main composition of P_i, represented the largest proportion of P in the NaOH-EDTA extracts, and increased from 65.4% to 87.4% in DC-1 and 74.2%–95.6% in DC-2 with sediment depth. A number of other P compounds, including monoesters, diesters, and phosphonates, generally decreased with sediment depth. Monoesters were the major forms of NaOH-EDTA P_o in these extracts. These monoesters included four stereoisomers of inositol hexakisphosphate (*myo*-, *scyllo*-, *neo*-, and *chiro*-IHP), other inositol phosphates (D-*myo*-ITP), degradation products of diester (α- and β-glycerophosphate, mononucleotides), sugar bound phosphate (glucose-6-phosphate and glucose-1-phosphate), choline phosphate, and a prominent, other unidentified monoesters. Within unhydrolyzed diesters, phospholipids and DNA were detected. A small amount of pyrophosphate in sediments from DC-1 and DC-2 was detected, which decreased quickly with depth increasing. Polyphosphate was not detected, which probably due to its breakdown to pyrophosphate (Sundareshwar et al., 2001; Hupfer et al., 2004). Additionally, trace amounts of phosphonates were observed in the NaOH-EDTA extracts.

3.6. Desorption and hydrolysis of P compounds adsorbed by minerals

A large amount of model P_o compounds and condensed P, especially IHP, was adsorbed by the minerals of goethite and montmorillonite, to form mineral-P complexes (Fig. S9). Contents of P_o or condensed P in mineral-P complexes were several times of contents of NaOH-EDTA P_o in sediments of Lake Dianchi (Fig. 1). However, 9.4–32.4% and 27.2–45.0% of labile monoester P including model P compounds of G6P, AMP, and *p*NPP adsorbed by goethite and montmorillonite could be desorbed from these complexes (Fig. 3a and Table S4). These desorbed labile monoester P would be easily hydrolyzed by enzymes in the solution (Fig. 3b). For condensed P, only small amounts (2.5%–3.4%) of pyrophosphates could be desorbed from the complexes (Fig. 3a, Table S4). The P remained in the minerals was extractable by NaOH, which recoveries of labile monoester P and condensed P in the experiments generally approach 100% (Table S4). These remaining P immobilized in the complexes were partially hydrolyzed by enzymes, though some immobilized labile monoester P and condensed P was hydrolyzed by enzyme-free buffer directly (Fig. 3c and d). Also, adsorption by goethite and montmorillonite protected some labile monoester P and condensed P from enzymatic hydrolysis (Fig. 3d and Table S4).

Few or no detectable IHP could be desorbed from complexes of G-IHP or M-IHP (Table S5). The IHP adsorbed by minerals even could not be totally extracted by NaOH (Table 2). Differences in concentrations of NaOH extractable IHP determined in buffer controls and after hydrolysis with phytase (Table 2) represented degradation of IHP by phytase, which was degraded to phosphate and extracted by NaOH. Few IHP in the G-IHP complex could be hydrolyzed by phytase even though the incubation time

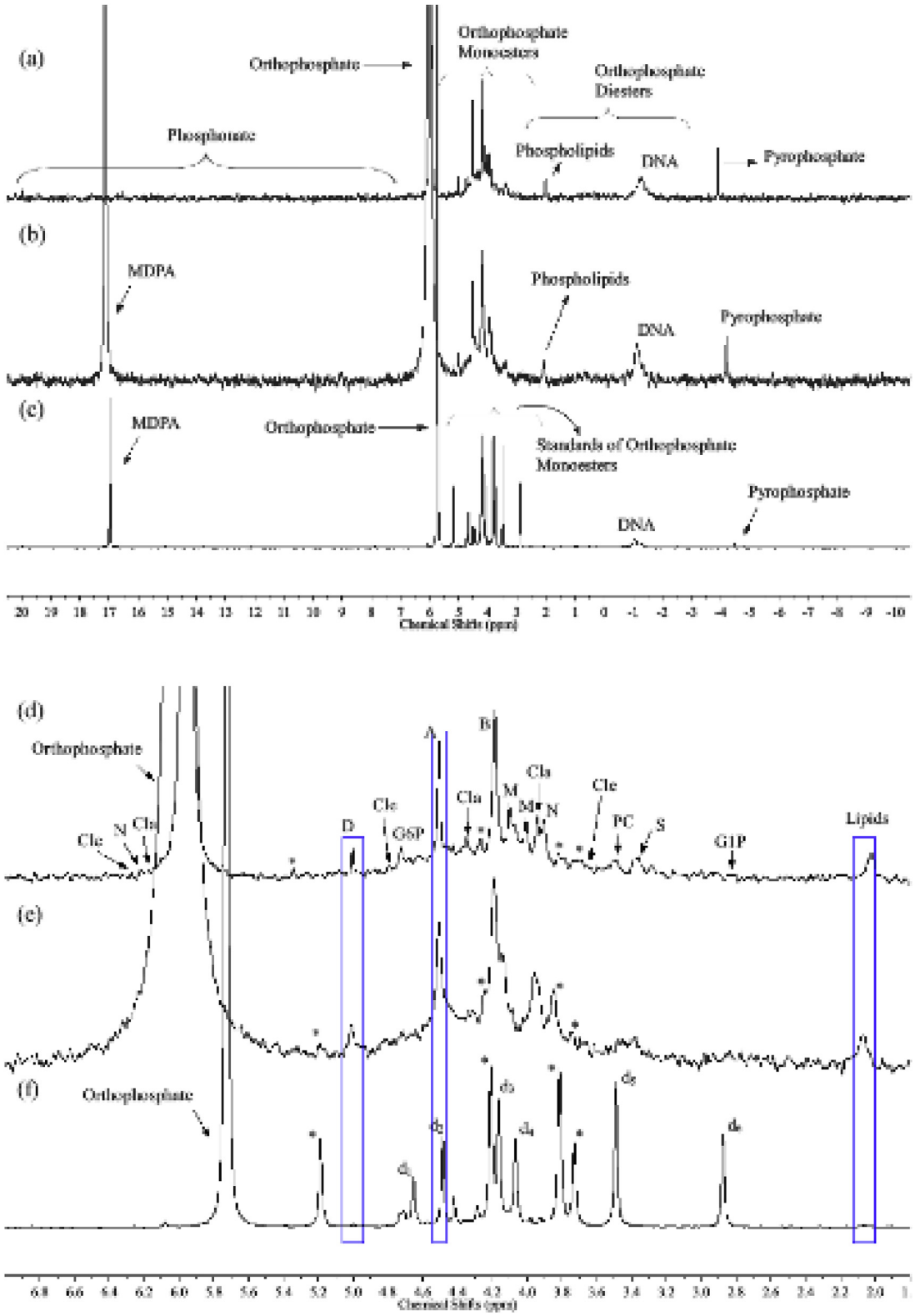

Fig. 2. ^{31}P NMR spectra of NaOH-EDTA P_o from sediments of Lake Dianchi and spiking experiment; (a), (b), (c), spectra including all peaks; (d), (e), (f), the region of monoester P. (a) and (d), sediment sample of DC-2 (1–2 cm); (b) and (e), surface sediment sample (X) from Lake Dianchi, NaOH-EDTA extractants adding MDPA (methylene diphosphonic acid); (c) and (f), NaOH-EDTA extractants of X adding a serious of P standards. The P standards: MDPA; DNA; *, *myo*-IHP (inositol hexakisphosphate); d_1, G6P (glucose-6-phosphate); d_2, α-Gly (α-glycerophosphate); d_3, β-Gly (β-glycerophosphate); d_4, AMP (adensine 5′ monophosphate); d_5, Pcho (choline phosphate); d_6, G1P (glucose-1-phosphate). Peak identified in the samples: Cle, *chiro*-IHP, 2e/4a; Cla, *chiro*-IHP, 4e/2a; *, *myo*-IHP, 4e/2a; N, *neo*-IHP; D, D-*myo*-ITP (D-*myo*-inositol 1,4,5 triphosphate); A, α-Gly; B, β-Gly; M, Ncu (mononucleotides); PC, Pcho; S, *scyllo*-IHP; G6P and G6P.

Table 1
Concentrations (mg kg^{-1}) and percentages (%) of NaOH-EDTA extractable P determined by ^{31}P NMR in sediments.

Sites	Depth	Organic P [a]												Inorganic P [a]		
		Monoesters									Unhydrolyzed diesters	Phosphonates		Ortho-P	Condense P	
		myo-IHP	*chiro*-IHP	*neo*-IHP	*scyllo*-IHP	D-*myo*-ITP	*α*-Gly	*β*-Gly	G6P	G1P	Nuc	Pcho	Unidentified	Lipid-P	DNA		Pyr	Poly
DC-1	1–2 cm	11.6 (2.1)[b]	17.0 (3.1)	6.2 (1.2)	3.6 (0.7)	2.1 (0.4)	13.0 (2.4)	25.9 (4.8)	4.5 (0.8)	0.6 (0.1)	28.2 (5.2)	2.0 (0.4)	28.2 (5.2)	1.6 (0.3)	35.1 (6.5)	0.3 (0.1)	354.3 (65.4)	7.7 (1.4)	0
	3–4 cm	7.7 (1.5)	12.8 (2.4)	6.2 (1.2)	3.1 (0.6)	1.6 (0.3)	9.7 (1.8)	18.0 (3.4)	2.7 (0.5)	0	13.2 (2.5)	2.2 (0.4)	30.7 (5.8)	2.2 (0.4)	20.6 (3.9)	0.3 (0.1)	392.5 (74.4)	4.4 (0.8)	0
	7–8 cm	5.9 (1.3)	9.7 (2.1)	1.4 (0.3)	2.3 (0.5)	1.6 (0.3)	5.1 (1.1)	9.9 (2.1)	1.9 (0.4)	0.1 (0.03)	4.9 (1.1)	0.8 (0.2)	36.9 (7.9)	1.7 (0.4)	10.9 (2.3)	0	372.1 (79.6)	1.9 (0.4)	0
	15–16 cm	3.2 (0.7)	6.1 (1.4)	1.3 (0.3)	0.4 (0.1)	1.0 (0.2)	1.1 (0.3)	1.8 (0.4)	0.6 (0.1)	0	2.0 (0.5)	0.4 (0.1)	29.8 (6.9)	2.3 (0.5)	3.0 (0.7)	0	378.9 (87.4)	1.5 (0.3)	0
DC-2	1–2 cm	11.6 (1.9)	15.1 (2.5)	6.1 (1.0)	3.4 (0.6)	1.5 (0.3)	11.4 (1.9)	20.6 (3.4)	3.0 (0.5)	0	18.3 (3.0)	2.7 (0.4)	30.9 (5.1)	1.2 (0.2)	24.1 (4.0)	1.8 (0.3)	450.6 (74.2)	4.6 (0.8)	0
	3–4 cm	18.0 (3.0)	22.2 (3.7)	7.8 (1.3)	3.2 (0.5)	2.6 (0.4)	11.8 (2.0)	19.1 (3.2)	3.6 (0.6)	0.1 (0.02)	17.0 (2.8)	2.9 (0.5)	12.7 (2.1)	3.0 (0.5)	22.1 (3.7)	0.3 (0.1)	449.9 (75.0)	3.1 (0.5)	0
	7–8 cm	7.4 (1.3)	11.1 (2.0)	5.4 (1.0)	3.3 (0.6)	1.1 (0.2)	4.7 (0.8)	7.6 (1.4)	2.6 (0.5)	0	7.5 (1.4)	0.4 (0.1)	41.4 (7.5)	2.4 (0.4)	5.2 (0.9)	0.6 (0.1)	450.0 (81.5)	1.6 (0.3)	0
	15–16 cm	3.2 (0.6)	6.2 (1.2)	2.1 (0.4)	0.3 (0.1)	0.5 (0.1)	0.9 (0.2)	3.3 (0.6)	1.1 (0.2)	0.5 (0.1)	2.1 (0.4)	0.4 (0.1)	33.5 (6.4)	1.3 (0.2)	0.8 (0.2)	1.1 (0.2)	467.3 (88.9)	1.1 (0.2)	0
	39–41 cm	1.7 (0.3)	3.1 (0.5)	0.5 (0.1)	0.1 (0.01)	0.2 (0.04)	0.7 (0.1)	0.7 (0.1)	0.4 (0.1)	0	1.6 (0.3)	0.3 (0.1)	13.2 (2.3)	0.6 (0.1)	1.4 (0.2)	0.5 (0.1)	558.6 (95.6)	1.1 (0.2)	0

[a] *myo*-IHP, *chiro*-IHP, *neo*-IHP, and *scyllo*-IHP, stereoisomers of inositol hexakisphosphate; *chiro*-IHP included *chiro*-IHP(2e/4a) and *chiro*-IHP(4e/2a) in Fig. 2; D-*myo*-ITP, D-*myo*-inositol 1,4,5 triphosphate; *α*-Gly, *β*-Gly, *α*- and *β*-glycerophosphate; G6P, G1P, glucose-6-phosphate and glucose-1-phosphate; Nuc, mononucleotides; Pcho, choline phosphate; Lipid-P, phospholipids; Ortho-P, orthophosphate; Pyr, pyrophosphate; Poly, polyphosphate.
[b] Values in parenthesis are percentages of individual P compounds in NaOH-EDTA extractable TP.

approached to 6 h at 55 °C. However, there was only approximately 10% of IHP in the M-IHP complex that could be hydrolyzed.

4. Discussion

4.1. Eutrophication of Lake Dianchi and source of organic matter in sediments

Comparison of the two sections of the cores showed an abrupt change in buck composition of organic matter in Section 2 (12–0 cm) relative to that in Section 1 (55–12 cm): this suggests that organic matter increased sharply in Section 2 in Lake Dianchi (Fig. S4). Based on the ^{137}Cs profiles recorded in sediments from area of DC-1 and DC-2 studied previously (Wang et al., 2009; Xiong et al., 2010), the sediment at 12 cm was accumulated during the 1970s. The TOC/TN ratio can be used to distinguish sources of organic matter in sediments. Plankton and bacteria generally have a TOC/TN ratio of between 4 and 10, whereas the TOC/TN ratio for vascular land plants is always greater than 20 (Meyers and Ishiwatari, 1993). The TOC/TN ratios in the sediments from Lake Dianchi are closer to the range for typical autochthonous sources than allochthonous sources (Fig. S4), a result which suggests that organic matter in sediments is mainly derived from algal and bacterial production in the lake water column. Phytoplankton in lacustrine environments has $\delta^{13}C$ values falling within the range of C3 land plants (with an average of −27‰) (Wang et al., 2009), and the $\delta^{15}N$ value of dissolved NO_3^- used by algae is typically 7–10‰ (Xiong et al., 2010). Thus, the conclusion was also further supported by $\delta^{13}C$ and $\delta^{15}N$ values in sediments from Lake Dianchi (Fig. S4). Therefore, variations in organic matter in sediment profiles indicated that there was a significant increase in the number of algae and bacteria from the 1970s onwards, which suggests that Lake Dianchi entered into a eutrophic stage or hyper-eutrophic stage in this period. This was also supported by the previous studies on the evolution of Lake Dianchi based on diatom (Gong et al., 2009), stable isotopes (Wang et al., 2009), and molecular compositions of organic matter (Xiong et al., 2010) recorded in sediments.

4.2. Geochemical records of P fractions during the evolution of Lake Dianchi

The trophic status of lakes can be determined by distribution of P in the profiles of sediments (Carey and Rydin, 2011). The distribution of P fractions (Fig. S6) in the profiles (except for the 4–0 cm of sediments), including TP, P_i, Fe/Al–P, and Ca–P were decreased with sediment depth, which further indicates that Lake Dianchi was eutrophic or hyper-eutrophic presently. The interpretation of P fractions in the sediment profiles of lakes is inherently difficult because of interactions of P sedimentation and the diagentic processes (Hupfer et al., 1995; Trolle et al., 2010; Carey and Rydin, 2011). Vertical distributions of P fractions (Fig. S6) were similar with long-term changes of TP in overlying water from Lake Dianchi (Zhu et al., 2015a), which may, however, suggest that the geochemical records of TP, P_i, Fe/Al–P, and Ca–P in the sediment profiles were closely related with the load of P in the overlying water, thus inputs of external P in Lake Dianchi (Gao et al., 2005), especially in the eutrophic or hyper eutrophic stage of Lake Dianchi (Section 2, 12–0 cm). Additionally, contents of TP and P_i (including Fe/Al–P and Ca–P) decreased in the sediments from 4 cm to 0 cm. This result corresponds with the TP decreasing in the water column after the year 2000, owing to a large extent, to the inputs of P being controlled (Lu et al., 2012; Zhu et al., 2015a). However, P_o was still accumulating in the sediments from 4 cm to 0 cm, which ongoing eutrophication of Lake Dianchi would continuously accumulate organic matter and P_o in the top sediments.

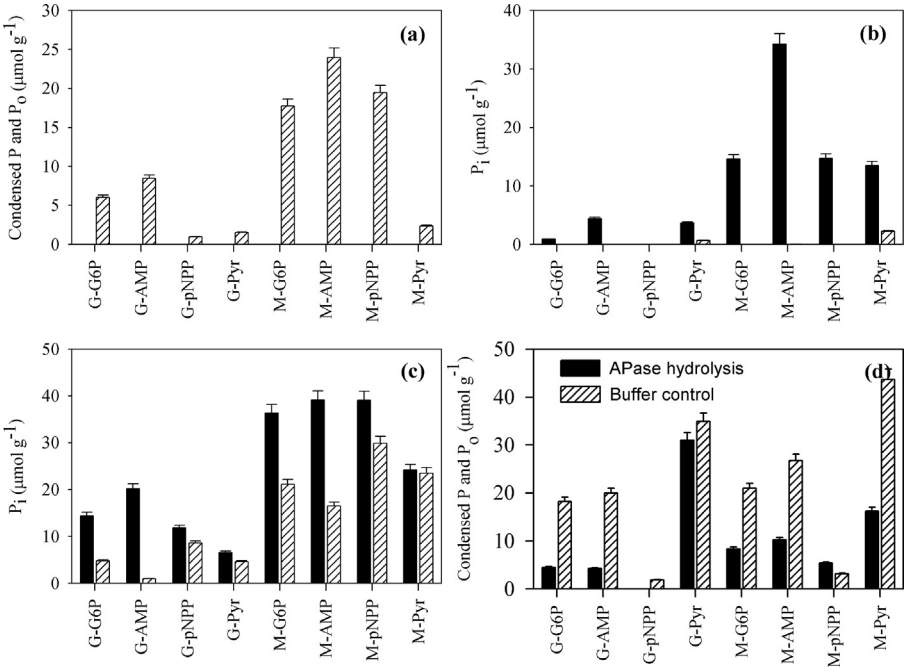

Fig. 3. Desorption and degradation of minerals-P complexes (G, goethite; M, montmorillonite; P including labile monoester P and condensed P) in the presence and absence of APase. (a), desorption of P_o and condensed P in the supernatants; (b), degradation of P_o and condensed P in the supernatants; (c), degradation of P_o and condensed P in the minerals-P complexes (NaOH extractable P); (d), unhydrolyzed P_o and condensed P in minerals-P complexes. Data are presented as the average value with standard deviation (n = 3).

Table 2
Unhydrolyzed IHP (μmol g^{-1}) in mineral-IHP complexes (NaOH extractable) after phytase hydrolysis.

Incubation time/complexes	G-IHP		M-IHP	
	Phytase hydrolysis	Buffer controls	Phytase hydrolysis	Buffer controls
2 h	133.8 ± 0.9 [a] (82.9) [b]	138.5 ± 0.9 (85.8)	143.5 ± 2.4 (55.1)	170.1 ± 1.7 (65.3)
6 h	129.0 ± 0.5 (79.9)	133.4 ± 6.2 (82.6)	138.4 ± 0.7 (53.1)	169.3 ± 3.2 (65.0)

[a] Concentration of IHP determined after degestion; Mean ± standard deviation (n = 3).
[b] Percentage (%) of IHP adsorbed on minerals (Fig. S9) extracted by NaOH.

Contents of metals including Fe, Al, and Ca would be important for diffusion or immobilization of P fractions in sediments. Variations of Al and Ca were similar with Fe/Al–P and Ca–P in sediment profiles, which contents decreased as the depth of sediment increased (Fig. S5). Al and Ca oxides were important P binding agents in sediments to bind the mobilized P in the water column (Carey and Rydin, 2011). First, the degradation of P_o accumulated in the sediments with primary production increasing would result in release of inorganic P immobilized by Al, Fe or Ca oxides (Carey and Rydin, 2011). The labile P diffused from the depth sediments would be possible adsorbed by Al, or Ca oxides in the surface sediments (Trolle et al., 2010; Carey and Rydin, 2011). Second, inputs of P increased as phosphate was mined in the area around Lake Dianchi, thus contents of P, Al, and Ca also increased (Figs. S5 and S6). Third, concentrations of TP increased sharply from 1970 to 2010 because of external P loads (Zhu et al., 2015a), therefore some P in the water column was adsorbed by sediments in Lake Dianchi. Although large inputs of external P loads and release of internal P were possibly adsorbed and accumulated in the surface sediments, the P concentrations in the water column were still high during the eutrophic or hyper eutrophic period of Lake Dianchi. Sediments in Section 2 (0–12 cm) may not be able to bind all mobilized P, which would result in release of P and sudden algal bloom outbreaks.

Distributions of Fe contents were significantly difference with Ca and Al contents in sediment profiles of Lake Dianchi (Fig. S5), which increased with sediment depth in Section 2. This suggests that the P associated with Fe was likely to be released simultaneously with eutrophication of lake. Based on the variation of P fractions in sediments before algal blooms and during algal blooms of Lake Dianchi, BD-P (bicarbonate dithionite, BD) can intensively be released to the overlying water and consequently promote algal blooms (Hu et al., 2007). It can be concluded that Fe and Fe–P in the sediments of Section 2 (0–12 cm) would be continuously released to the water column from the anoxic sediments because of the organic matter accumulation in the eutrophic stage of Lake Dianchi. Some P_o bound to reductive Fe in the depth sediment would be also released and diffused to the top sediments.

4.3. *Bioavailability and chemical structure of P_o in sediment profiles*

The depth attenuation of P_o in sediment profiles was generally attributed to the degradation of P_o during diagenetic processes (Wilson et al., 2010), such as Lake Taihu (Ding et al., 2013) and Lake Erken (Ahlgren et al., 2005; Reitzel et al., 2007). Based on the source of organic matter and significant correlations between NaOH-EDTA P_o and TOC in sediments, P_o in the sediments is mainly derived from autochthonous sources than allochthonous sources. The increase accumulation of TOC in sediments with eutrophication would also result in more accumulation of P_o in sediments of Lake Dianchi, which due to the sediment rate of P_o far exceeded its

mineralization degree (Gao et al., 2010; Zhu et al., 2013b). Therefore, the depth attenuation of NaOH-EDTA P_o in the sediment profiles is likely the net result of the increasing accumulation of organic matter and degradation during sediment.

The depth attenuation of bioavailable P_o characterized by enzymatic hydrolysis in these sediment profiles were consistent with depth attenuation of biogenic P (e.g., monoester P, diester P, and pyrophosphate) characterized by ^{31}P NMR in the sediments profiles from other lakes, such as Lake Erken (Ahlgren et al., 2005) and Lake Taihu (Ding et al., 2013). Compared with bioavailable labile monoester P, bioavailable diester P is likely to be degraded quickly in the sediment profiles (Fig. 1). This is supported by that the half-life of diester P was shorter than that of monoester P in the sediments of lakes (Ahlgren et al., 2005; Ding et al., 2013).

Based on results of ^{31}P NMR analysis and enzymatic hydrolysis, P species and their bioavailability in NaOH-EDTA extracts were compared directly (Table 3). In general, contents of total P_o determined by molybdate colorimetry were approximately 30% greater than those measured by use of ^{31}P NMR (Table 3). For enzymatic hydrolysis, total P_o was determined by molybdate colorimetry combined with $K_2S_2O_8$ digestion, which would overestimate the contents due to the association of orthophosphate with organic matter (Turner et al., 2006; Zhu et al., 2015b). Hydrolysis of labile P_o during ^{31}P NMR analysis would amplify these differences (Turner et al., 2003; Cade-Menun et al., 2006). Differences between contents of total P_o determined by molybdate colorimetry and ^{31}P NMR generally decreased with sediment depth. This result implies that more labile P_o is likely to be hydrolyzed during ^{31}P NMR analysis in the surface sediments. More accumulation of organic matter in the surface sediments would also result in combination of orthophosphate with organic matter. Labile monoester P and condensed P identified by ^{31}P NMR could be hydrolyzed by enzymes, except for some samples form the surficial sediments (Table 3). Compared with ^{31}P NMR analysis, enzymatic hydrolysis provided a relatively mild approach for characterizing labile P_o (He et al., 2006). Therefore, large amounts of mononucleotides identified in the ^{31}P NMR spectra in surficial sediments (Table 1), could be products of degradation of RNA (Turner et al., 2003; Cade-Menun et al., 2006). In some samples, concentrations of diesters characterized by enzymatic hydrolysis were greater than those characterized by ^{31}P NMR (Table 3). Because P species characterized by enzymatic hydrolysis was calculated as the difference in the presence and absence of enzymes, which would also produce more variable results (He et al., 2007; Jarosch et al., 2015). Therefore, some comparisons, such as diester P, should be careful. However, it is apparent that few or no phytate-like P have been detected by enzymatic hydrolysis though a significant contents of inositol phosphates characterized by ^{31}P NMR (Tables 1 and 3). Generally, NaOH-EDTA P_o could not be completely hydrolyzed by these enzymes. There were only 42.9–72.5% in DC-1 and 43.5–100% in DC-2 of P_o determined by molybdate colorimetry, 54.8–70.4% in DC-1 and 54.6–100% in DC-2 measured by ^{31}P NMR that could be hydrolyzed by these enzymes. Some P species, especially phytate or phytate-like P, characterized by ^{31}P NMR would be combined with other organic matter, such as humic acid and fulvic acid or/and metals ions (e.g., Al^{3+}, Ca^{2+} and Fe^{3+}) to form the complexes of P_o-metal-organic matter or P_o-organic matter, which would be resistant to hydrolysis by these enzymes (He et al., 2015; Jarosch et al., 2015; Zhu et al., 2015b). This mechanism can be a significant factor determining the bioavailability and preservation of P_o in sediments (Zhu et al., 2015b). Contents of P_o that are resistant to enzymatic hydrolysis significantly decreased with sediment depth (Table 3). These results further indicated that the interaction between P_o and other organic matter would be an important factor for preservation of P_o in the sediment profiles.

In order to better understand bioavailability and preservation of P_o in sediments, the residual P_o in the ERP was further investigated. The results of sequential extraction (Table S3) and ^{31}P NMR spectra of ERP (Fig. S7) indicated that the majority of P_o and condensed P in sediments was extracted by NaOH-EDTA extractants. Some phosphate in the ERP is likely associated with organic matter, which is not detectable by use of molybdate colorimetry (Turner et al., 2006; Zhu et al., 2015b). Thus, some phosphate would be considered as a portion of P_o, which overestimated the proportion of P_o in extracts. Few studies have discussed residue P after extraction with NaOH-EDTA followed by ^{31}P NMR analysis (Cade-Menun et al., 2005, 2015). Residual P after extraction with NaOH-EDTA was further analyzed by solid ^{31}P NMR in marine particulates during a previous study, which also showed that the majority of P remaining in residues was orthophosphate (Cade-Menun et al., 2005). In these lake sediments, aggregative results showed that P_o determined by the SMT protocol is likely overestimated. Especially, overestimation of

Table 3
Comparison of P species and bioavailability (mg kg^{-1}) in NaOH-EDTA extracts identified by ^{31}P NMR analysis and enzymatic hydrolysis in the sediment profiles.

Sites	Depth	Molybdate colorimetry	^{31}P NMR				Enzymatic hydrolysis			
		Total P_o [a]	Total P_o [a]	LM and condensed P [b]	Unhydrolyzed diester P	Inositol phosphates [c]	LM and condensed P	Diester P	Phytate-like P	Total hydrolyzable P [d]
DC-1	1–2 cm	242.6 ± 5.6 [e]	187.5	81.9	36.7	40.4	61.6 ± 3.4	43.8 ± 1.0	0.9 ± 0.4	106.3 ± 7.1
	3–4 cm	180.7 ± 0.4	135.3	50.2	22.8	31.2	41.3 ± 5.5	36.2 ± 6.0	- [f]	77.5 ± 6.0
	7–8 cm	121.0 ± 5.0	95.1	24.7	12.6	20.9	21.6 ± 3.2	15.3 ± 13.3	15.2 ± 6.7	52.1 ± 5.6
	15–16 cm	53.0 ± 2.7	54.6	7.4	5.3	12.0	22.9 ± 8.9	15.5 ± 12.7	–	38.4 ± 2.7
DC-2	1–2 cm	211.4 ± 32.0	156.5	60.8	25.2	37.7	89.9 ± 1.9	27.9 ± 6.3	–	117.8 ± 9.1
	3–4 cm	187.7 ± 14.4	149.6	57.8	25.1	53.9	69.3 ± 17.4	12.4 ± 8.2	–	81.7 ± 13.0
	7–8 cm	110.5 ± 0.7	102.3	24.4	7.6	28.3	30 ± 3.9	9.9 ± 4.1	18.8 ± 8.3	58.7 ± 22.6
	15–16 cm	45.9 ± 0.2	58.5	9.4	2.1	12.3	33.6 ± 15.8	19.4 ± 14.1	–	53.0 ± 4.1
	39–41 cm	39.8 ± 18.8	26.1	4.8	2.0	5.6	10.3 ± 6.5	19.9 ± 12.0	–	30.2 ± 5.0

[a] These total P_o includes condensed P.
[b] LM: labile monoester P. LM identified in ^{31}P NMR spectra including α-Gly, β-Gly, G6P, G1P, F6P, Nuc, and Pcho in Table 1.
[c] Inositol phosphates includes *myo*-IHP, *chiro*-IHP, *neo*-IHP, and *scyllo*-IHP, and D-*myo*-ITP.
[d] The greatest contents of P hydrolyzed by enzymes.
[e] Mean ± standard deviation (n = 3).
[f] "-" data not detected or negative value.

P_o contents would be greater in the deeper sediments (Tables S1 and S2). It is likely that some P_i immobilized strongly with minerals (e.g., P_i migrated into particle interiors) during diagenesis (Ruttenberg and Sulak, 2011), which results in the solution of HCl could not recover all P_i from sediments in the SMT protocol. And then the remaining P_i in sediments would be sequentially detected as P_o after ignition and extraction by HCl solution again (Ruban et al., 1999, 2001). Similarly, this ignition method trends to overestimate the contents of P_o in most soils by increasing the solubility of P_i from the samples following ignition (Condron et al., 1990; Turner et al., 2005). Accurate estimation of P_o contents in the sediments is important for understanding of biogeochemical cycling of P_o in lakes. Thus, investigation of total P_o by use of multiple methods in additional sediments of lakes is needed. Additionally, the finial non-extractable P after NaOH-EDTA and ERP were possibly inert P_i or phosphonates that would be preserved in sediments (Cade-Menun et al., 2005).

4.4. Influence of minerals on bioavailability and preservation of model P compounds

Incorporation of P_o compounds and condensed P into organic matter or complexes with metal ions is a factor that influences the bioavailability and preservation of P_o in sediments (Laarkamp, 2000; Zhu et al., 2015b). However, P extractable by NaOH-EDTA includes a range of P_o or condensed P adsorbed in sediments by minerals, such as ion oxides, aluminum oxides, and calcium oxides. Therefore, some bioavailable P_o characterized by enzymatic hydrolysis and solution ^{31}P NMR that was extractable with NaOH-EDTA (Fig. 1, Tables 1 and 2) would likely have been immobilized in sediments *in situ*. For labile monoester P, they were loosely adsorbed by minerals, which could be released from sediments easily, thus being hydrolyzed by enzymes (Fig. 3a and b). Condensed P, such as pyrophosphates, is good complexing agents for metals, thus they would combine strongly with minerals. Glucose-1-phosphate (G1P) adsorbed on the goethite surface could be hydrolyzed by acid phosphatase directly (Olsson et al., 2011). However, released carbon goes to the solution whereas orthophosphate remains adsorbed on goethite (Olsson et al., 2011). Therefore, except for desorption, the labile monoester P and condensed P adsorbed on the surface of minerals could be possibly hydrolyzed by phosphatase directly (Fig. 3c and d), and then transformed to P_i form directly, such as Fe or Al bound P_i. Alternatively, results also showed that enzymatic hydrolysis of some labile monoester P or condensed P adsorbed by minerals would be decelerated or inhibited referring to free P compounds (Fig. 3d). Inositol hexakisphosphate is strongly adsorbed by minerals like oxides, hydrous oxides and hydroxides of Fe and Al, which accumulate in environments, such as soils or sediments (Turner et al., 2002; Johnson et al., 2012). For adsorption of IHP by some minerals such as Al oxides, it was hardly be bioavailable for organisms in sediments (Tables 2 and S5). This is also supported by the results of a previous study (Giaveno et al., 2010). Also, desorption of IHP with dissolution of Fe oxides under anoxic conditions would hydrolyzed by phytase. Thus, bioavailability of IHP adsorbed on minerals seems to be governed by mineral composition (Giaveno et al., 2010). Generally, minerals have been indicated to protect the majority of adsorbed IHP from enzymatic hydrolysis. Therefore, they would trend to be preserved in sediments (Turner and Weckström, 2009). Immobilization by minerals could be another important mechanism influencing bioavailability and preservation of P_o during eutrophication of lakes.

4.5. Biogeochemical cycling of organic phosphorus and its role in eutrophication

Blooming of algae and cyanobacteria associated with cultural eutrophication is a primary driver of nutrients cycling such as P (Cottingham et al., 2015). Results of this study demonstrated that biogeochemical cycling of P was active in the sediments accumulated from eutrophic periods of Lake Dianchi (Section 2: 12–0 cm). Ratios of NaOH-EDTA P_o and bioavailable P_o to Fe/Al–P decreased significantly with sediment depths during the periods of eutrophication of Lake Dianchi, which became stable and varied in a narrow range in sediments from Section 1 (Fig. 4). Fe/Al–P can be used as an index of algae-available and bioactive P_i (Zhu et al., 2013a). The depth attenuation of these ratios is most likely attributed to the degradation of P_o and release of Fe–P with sediment depths. Blooming of phytoplankton and accumulation of organic matter in sediments is also likely accelerating transformation of bioactive P_i to P_o and bioavailable P_o. Reference to the constant ratios of NaOH-EDTA P_o and bioavailable P_o to Fe/Al–P in sediments

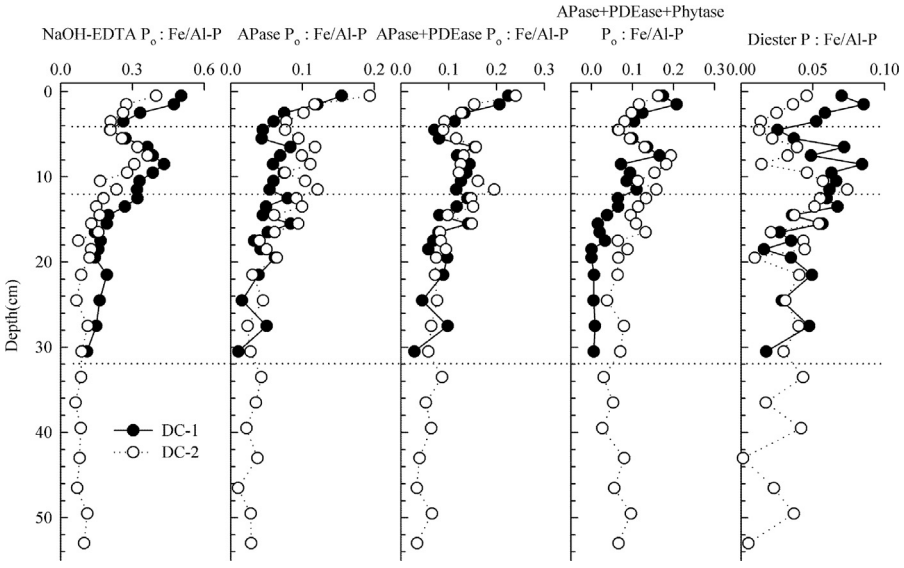

Fig. 4. Ratios (w/w) of P_o and enzymatically hydrolysable P_o (bioavailable P_o) to Fe/Al–P in sediment profiles of Lake Dianchi.

from Section 1 (55–12 cm), the bioavailable P_o, especially in the top 4 cm sediments (Fig. 4), would be a large potentially sources of bioavailable P for algal blooming. Especially, bioavailability of labile monoester P was less influenced by other organic matter and minerals. Most of labile monoester P would be available to be recycled to support ongoing blooming of algae. Some labile monoester P that was precipitated in sediments by minerals would be degraded to minerals bonded P_i directly, such as Fe/Al–P, to be released from sediments or preserved in sediments. Therefore, these types of cycling of bioavailable P_o could potentially maintain the eutrophic status of lakes for long periods, even after the control of external P inputs and lack of internal bioavailable P_i in the sediments (Carpenter et al., 1999; Zhu et al., 2013b). Without continued intervention to break this cycle, the eutrophic status of lakes and concomitant blooming of phytoplankton would persist indefinitely. Insight derived from this work and others (Laarkamp, 2000; Zhu et al., 2015b) in which enzymatic hydrolysis and ^{31}P NMR characterization have shown that some P_o, especially phytate-like P, would be preserved in sediments, which can be enhanced by the minerals (e.g., Al oxides) and other organic matter (e.g., humic acid). However, it was likely lack of binding agents (such as Fe, Al and Ca) for P in the eutrophic stage of Lake Dianchi. Therefore, continued intervention should be done to promote the preservation of more bioavailable P_o and the capture of released P_i in the sediments. Aluminum hydroxide has been used to precipitate P from water column and to immobilize P in the sediment in more than 200 lakes worldwide (Jensen et al., 2015). This has accelerated preservation of P_o from surface waters of eutrophic lakes in their sediments. Therefore, precipitation of P is likely key factor in preservation of P by sequestration in sediments that will accelerate reversing the trophic status of lakes.

5. Conclusions

Two sections of evolution process of Lake Dianchi was identified by the sediment profiles: eutrophic or hyper eutrophic stage (Section 2: 12–0 cm); oligotrophic stage and mesotrophic stage (Section 1: 55–12 cm). Majority of P_o and condensed P in these sediments was extracted by NaOH-EDTA extractants. The residual P after NaOH-EDTA extraction was mainly composition of Ortho-P. The contents of P_o would be overestimated by SMT protocol (ignition method) in sediments of lakes, especially in the depth sediments. Thus, bioavailability and preservation of these NaOH-EDTA P_o could provide key information for biogeochemical cycling of P_o in sediments of Lake Dianchi.

With eutrophication of Lake Dianchi, accumulation of organic matter and P_o in sediments was increasing. Enzymatically hydrolysable P_o, thus degradable and bioavailable P_o, was also increasing accumulation in sediments from eutrophic or hyper eutrophic stage of Lake Dianchi. Based on ^{31}P NMR, 54.8–70.9% in DC-1 and 54.7–100% in DC-2 identified and unidentified P_o could be hydrolyzed by the phosphatase. Interaction between P_o and other organic matter was an important mechanism for some P_o resistant to enzymatic hydrolysis, thus potentially preserved in the sediment profiles for a longer period. Immobilization of P_o by minerals was also an important mechanism for P_o resistant to be hydrolyzed by phosphatase, thus preserved in the sediment profiles.

The transformations between bioavailable P_o and Fe/Al–P were active with eutrophication of Lake Dianchi. Bioavailable P_o will have played an important role in maintain the eutrophic status of lakes as external inputs of P have been largely controlled. Though large of phytate-like P was likely preserved in sediments, bioavailable labile monoester P and diester P would be active and recycled to support ongoing blooming of algae. Treatments such as adding Al hydroxide could be utilized to accelerate preservation of some P_o from surface waters of eutrophic lakes in their sediments.

Acknowledgments

This research was jointly supported by the National Natural Science Foundation of China (No. 41630645, 41521003, 41573126).

Appendix A. Supplementary data

Supplementary data related to this article can be found at https://doi.org/10.1016/j.chemosphere.2018.07.134.

References

Ahlgren, J., Tranvik, L., Gogoll, A., Waldebäck, M., Markides, K., Rydin, E., 2005. Sediment depth attenuation of biogenic phosphorus compounds measured by ^{31}P NMR. Environ. Sci. Technol. 39, 867–872.
Atkinson, R.J., Posner, A.M., Quirk, J.P., 1967. Adsorption of potential-determining ions at the ferric oxide-aqueous electrolyte interface. J. Phys. Chem. 71, 550–558.
Bünemann, E.K., 2008. Enzyme additions as a tool to assess the potential bioavailability of organically bound nutrients. Soil Biol. Biochem. 40, 2116–2129.
Cade-Menun, B.J., 2015. Improved peak identification in ^{31}P-NMR spectra of environmental samples with a standardized method and peak library. Geoderma 257–258, 102–114.
Cade-Menun, B.J., Benitez-Nelson, C.R., Pellechia, P., Paytan, A., 2005. Refining ^{31}P nuclear magnetic resonance spectroscopy for marine particulate samples: storage conditions and extraction recovery. Mar. Chem. 97, 293–306.
Cade-Menun, B.J., He, Z., Zhang, H., Endale, D.M., Schomberg, H.H., Liu, C.W., 2015. Stratification of phosphorus forms from long-term conservation tillage and poultry litter application. Soil Sci. Soc. Am. J. 79, 504–516.
Cade-Menun, B.J., Navaratnam, J.A., Walbridge, M.R., 2006. Characterizing dissolved and particulate phosphorus in water with ^{31}P nuclear magnetic resonance spectroscopy. Environ. Sci. Technol. 40, 7874–7880.
Carey, C.C., Rydin, E., 2011. Lake trophic status can be determined by the depth distribution of sediment phosphorus. Limnol. Oceanogr. 56, 2051–2063.
Carpenter, S.R., Ludwig, D., Brock, W.A., 1999. Management of eutrophication for lakes subject to potentially irreversible change. Ecol. Appl. 9, 751–771.
Chen, M., Ding, S., Chen, X., Sun, Q., Fan, X., Lin, J., Ren, M., Yang, L., Zhang, C., 2018. Mechanisms driving phosphorus release during algal blooms based on hourly changes in iron and phosphorus concentrations in sediments. Water Res. 133, 153–164.
Condron, L.M., Moir, J.O., Tiessen, H., Stewart, J.W.B., 1990. Critical evaluation of methods for determining total organic phosphorus in tropical soils. Soil Sci. Soc. Am. J. 54, 1261–1266.
Conley, D.J., Paerl, H.W., Howarth, R.W., Boesch, D.F., Seitzinger, S.P., Havens, K.E., Lancelot, C., Likens, G.E., 2009. Controlling eutrophication: nitrogen and phosphorus. Science 323, 1014–1015.
Cottingham, K.L., Ewing, H.A., Greer, M.L., Carey, C.C., Weathers, K.C., 2015. Cyanobacteria as biological drivers of lake nitrogen and phosphorus cycling. Ecosphere 6, 1.
Ding, S., Chen, M., Gong, M., Fan, X., Qin, B., Xu, H., Gao, S., Jin, Z., Tsang, D.C.W., Zhang, C., 2018. Internal phosphorus loading from sediments causes seasonal nitrogen limitation for harmful algal blooms. Sci. Total Environ. 625, 872–884.
Ding, S., Xu, D., Bai, X., Yao, S., Fan, C., Zhang, C., 2013. Speciation of organic phosphorus in a sediment profile of Lake Taihu II. Molecular species and their depth attenuation. J. Environ. Sci. 25, 925–932.
Ding, S.M., Fan, X., Zhang, C., 2010. Caution needed in pretreatment of sediments for refining Phosphorus-31 nuclear magnetic resonance analysis: results from a comprehensive assessment of pretreatment with ethylenediaminetetraacetic acid. J. Environ. Qual. 39, 1668–1678.
Gao, H., Liu, T., Zhu, F., Deng, L., 2010. Characteristics of organic phosphorus in sediments of Lake Dianchi, China. Fresenius Environ. Bull. 19, 3125–3130.
Gao, L., Zhou, J.M., Yang, H., Chen, J., 2005. Phosphorus fractions in sediment profiles and their potential contributions to eutrophication in Dianchi Lake. Environ. Geol. 48, 835–844.
Giaveno, C., Celi, L., Richardson, A.E., Simpson, R.J., Barberis, E., 2010. Interaction of phytases with minerals and availability of substrate affect the hydrolysis of inositol phosphates. Soil Biol. Biochem. 42, 491–498.
Giles, C.D., Lee, L.G., Cade-Menun, B.J., Hill, J.E., Isles, P.D.F., Schroth, A.W., Druschel, G.K., 2015. Characterization of organic phosphorus form and bioavailability in lake Sediments using P Nuclear magnetic resonance and enzymatic hydrolysis. J. Environ. Qual. 44, 882–894.
Golterman, H., Paing, J., Serrano, L., Gomez, E., 1998. Presence of and phosphate release from polyphosphates or phytate phosphate in lake sediments. Hydrobiologia 364, 99–104.
Golterman, H.L., 1996. Fractionation of sediment phosphate with chelating compounds: a simplification, and comparison with other methods. Hydrobiologia 335, 87–95.

Gong, Z., Li, Y., Shen, J., Xie, P., 2009. Diatom community succession in the recent history of a eutrophic Yunnan Plateau lake, Lake Dianchi, in subtropical China. Limnology 10, 247–253.
He, Z., Cade-Menun, B.J., Toor, G.S., Fortuna, A.M., Honeycutt, C.W., Sims, J.T., 2007. Comparison of phosphorus forms in wet and dried animal manures by solution Phosphorus-31 nuclear magnetic resonance spectroscopy and enzymatic hydrolysis. J. Environ. Qual. 36, 1086–1095.
He, Z., Honeycutt, C.W., 2001. Enzymatic characterization of organic phosphorus in animal manure. J. Environ. Qual. 30, 1685–1692.
He, Z., Tazisong, I.A., Senwo, Z.N., 2015. Forms and lability of phosphorus in humic and fulvic acids. In: He, Z., Wu, F. (Eds.), Labile Organic Matter-chemical Compositions, Function, and Significance in Soil and the Environment. Soil Sci. Soc. Am., Madison, WI, p. 10.2136/sssaspecpub2162.2014.0035.
He, Z., Toor, G.S., Honeycutt, C.W., Sims, J.T., 2006. An enzymatic hydrolysis approach for characterizing labile phosphorus forms in dairy manure under mild assay conditions. Bioresour. Technol. 97, 1660–1668.
Herbes, S.E., Allen, H.E., Mancy, K.H., 1975. Enzymatic characterization of soluble organic phosphorus in lake water. Science 187, 432.
Hu, J., Shen, Q., Liu, Y., Liu, J., 2007. Mobility of different phosphorus pools in the sediment of Lake Dianchi during cyanobacterial blooms. Environ. Monit. Assess. 132, 141–153.
Hupfer, M., Gächter, R., Giovanoli, R., 1995. Transformation of phosphorus species in settling seston and during early sediment diagenesis. Aquat. Sci. 57, 305–324.
Hupfer, M., Rübe, B., Schmieder, P., 2004. Origin and diagenesis of polyphosphate in lake sediments: a ^{31}P-NMR study. Limnol. Oceanogr. 49, 1–10.
Jarosch, K.A., Doolette, A.L., Smernik, R.J., Tamburini, F., Frossard, E., Bünemann, E.K., 2015. Characterisation of soil organic phosphorus in NaOH-EDTA extracts: a comparison of ^{31} P NMR spectroscopy and enzyme addition assays. Soil Biol. Biochem. 91, 298–309.
Jensen, H.S., Reitzel, K., Egemose, S., 2015. Evaluation of aluminum treatment efficiency on water quality and internal phosphorus cycling in six Danish lakes. Hydrobiologia 751, 189–199.
Johnson, B.B., Quill, E., Angove, M.J., 2012. An investigation of the mode of sorption of inositol hexaphosphate to goethite. J. Colloid Interface Sci. 367, 436–442.
Laarkamp, K.L., 2000. Organic Phosphorus in Marine Sediments: Chemical Structure, Diagenetic Alteration, and Mechanisms of Preservation. Massachusetts Institute of Technology/Woods Hole Ocenographic Institution, pp. 167–173.
Lu, J., Wang, H., Pan, M., Xia, J., Xing, W., Liu, G., 2012. Using sediment seed banks and historical vegetation change data to develop restoration criteria for a eutrophic lake in China. Ecol. Eng. 39, 95–103.
Meyers, P.A., Ishiwatari, R., 1993. Lacustrine organic geochemistry–an overview of indicators of organic matter sources and diagenesis in lake sediments. Org. Geochem. 20, 867–900.
Monbet, P., McKelvie, I.D., Saefumillah, A., Worsfold, P.J., 2007. A protocol to assess the enzymatic release of dissolved organic phosphorus species in waters under environmentally relevant conditions. Environ. Sci. Technol. 41, 7479–7485.
Murphy, J., Riley, J.P., 1962. A modified single solution method for the determination of phosphate in natural waters. Anal. Chim. Acta 27, 31–36.
Olsson, R., Giesler, R., Loring, J.S., Persson, P., 2011. Enzymatic hydrolysis of organic phosphates adsorbed on mineral surfaces. Environ. Sci. Technol. 46, 285–291.
Reasoner, M.A., 1993. Equipment and procedure improvements for a lightweight, inexpensive, percussion core sampling system. J. Paleolimnol. 8, 273–281.
Reitzel, K., Ahlgren, J., DeBrabandere, H., Waldebäck, M., Gogoll, A., Tranvik, L., Rydin, E., 2007. Degradation rates of organic phosphorus in lake sediment. Biogeochemistry 82, 15–28.
Reitzel, K., Ahlgren, J., Gogoll, A., Rydin, E., 2006. Effects of aluminum treatment on phosphorus, carbon, and nitrogen distribution in lake sediment: a ^{31}P NMR study. Water Res. 40, 647–654.
Ruban, V., Brigault, S., Demare, D., Philippe, A.M., 1999. An investigation of the origin and mobility of phosphorus in freshwater sediments from Bort-Les-Orgues Reservoir, France. J. Environ. Monit. 1, 403–407.
Ruban, V., López-Sánchez, J.F., Pardo, P., Rauret, G., Muntau, H., Quevauviller, P., 2001. Harmonized protocol and certified reference material for the determination of extractable contents of phosphorus in freshwater sediments - a synthesis of recent works. Fresen. J. Anal. Chem. 370, 224–228.
Ruttenberg, K.C., Sulak, D.J., 2011. Sorption and desorption of dissolved organic phosphorus onto iron (oxyhydr) oxides in seawater. Geochim. Cosmochim. Acta 75, 4095–4112.
Schindler, D.W., 1977. Evolution of phosphorus limitation in lakes. Science 195, 260–262.
Smith, V.H., Schindler, D.W., 2009. Eutrophication science: where do we go from here? Trends Ecol. Evol. 24, 201–207.
Sneddon, J., Hardaway, C., Bobbadi, K.K., Reddy, A.K., 2006. Sample preparation of solid samples for metal determination by atomic spectroscopy—an overview and selected recent applications. Appl. Spectrosc. Rev. 41, 1–14.
Sundareshwar, P.V., Morris, J.T., Pellechia, P.J., Cohen, H.J., Porter, D.E., Jones, B.C., 2001. Occurrence and ecological implications of pyrophosphate in estuaries. Limnol. Oceanogr. 46, 1570–1577.
Trolle, D., Hamilton, D.P., Pilditch, C.A., 2010. Evaluating the influence of lake morphology, trophic status and diagenesis on geochemical profiles in lake sediments. Appl. Geochem. 25, 621–632.
Turner, B.L., Cade-Menun, B.J., Condron, L.M., Newman, S., 2005. Extraction of soil organic phosphorus. Talanta 66, 294–306.
Turner, B.L., Mahieu, N., Condron, L.M., 2003. Phosphorus-31 nuclear magnetic resonance spectral assignments of phosphorus compounds in soil NaOH-EDTA extracts. Soil Sci. Soc. Am. J. 67, 497–510.
Turner, B.L., Newman, S., Reddy, K.R., 2006. Overestimation of organic phosphorus in wetland soils by alkaline extraction and molybdate colorimetry. Environ. Sci. Technol. 40, 3349–3354.
Turner, B.L., Papházy, M.J., Haygarth, P.M., McKelvie, I.D., 2002. Inositol phosphates in the environment. Philos. Trans. R. Soc. Lond. B Biol. Sci. 357, 449–469.
Turner, B.L., Weckström, K., 2009. Phytate as a novel phosphorus-specific paleoindicator in aquatic sediments. J. Paleolimnol. 42, 391–400.
Vestergren, J., Vincent, A.G., Jansson, M., Persson, P., Ilstedt, U., Gröbner, G., Giesler, R., Schleucher, J., 2012. High-resolution characterization of organic phosphorus in soil extracts using 2D ^{1}H-^{31}P NMR correlation spectroscopy. Environ. Sci. Technol. 46, 3950–3956.
Wang, F.S., Liu, C., Wu, M., Yu, Y., Wu, F., Lü, S., Wei, Z., Xu, G., 2009. Stable isotopes in sedimentary organic matter from Lake Dianchi and their indication of eutrophication history. Water Air Soil Pollut. 199, 159–170.
Wilson, T.A., Amirbahman, A., Norton, S.A., Voytek, M.A., 2010. A record of phosphorus dynamics in oligotrophic lake sediment. J. Paleolimnol. 44, 279–294.
Worsfold, P.J., Monbet, P., Tappin, A.D., Fitzsimons, M.F., Stiles, D.A., McKelvie, I.D., 2008. Characterisation and quantification of organic phosphorus and organic nitrogen components in aquatic systems: a review. Anal. Chim. Acta 624, 37–58.
Xiao, D., Pan, B., Wu, M., Liu, Y., Zhang, D., Peng, H., 2012. Sorption comparison between phenanthrene and its degradation intermediates, 9,10-phenanthrenequinone and 9-phenanthrol in soils/sediments. Chemosphere 86, 183–189.
Xiong, Y., Wu, F., Fang, J., Wang, L., Li, Y., Liao, H., 2010. Organic geochemical record of environmental changes in Lake Dianchi, China. J. Paleolimnol. 44, 217–231.
Zhang, R., Wu, F., He, Z., Zheng, J., Song, B., Jin, L., 2009. Phosphorus composition in sediments from seven different trophic lakes, China: a Phosphorus-31 NMR study. J. Environ. Qual. 38, 353–359.
Zhang, R., Wu, F., Liu, C., Fu, P., Li, W., Wang, L., Liao, H., Guo, J., 2008. Characteristics of organic phosphorus fractions in different trophic sediments of lakes from the middle and lower reaches of Yangtze River region and Southwestern Plateau, China. Environ. Pollut. 152, 366–372.
Zhang, X., Wang, Y., Lei, H., 1996. Authigenic mineralogy, depositional environments and evolution of fault-bounded lakes of the Yunnan Plateau, South-western China. Sedimentology 43, 367–380.
Zhu, M., Zhu, G., Li, W., Zhang, Y., Zhao, L., Gu, Z., 2013a. Estimation of the algal-available phosphorus pool in sediments of a large, shallow eutrophic lake (Taihu, China) using profiled SMT fractional analysis. Environ. Pollut. 173, 216–223.
Zhu, Y., Wu, F., He, Z., 2015a. Bioavailability and preservation of organic phosphorus in freshwater sediments and its role in lake eutrophication. In: He, Z., Wu, F. (Eds.), Labile Orgnaic Matter—chemical Composition, Function, and Significance in Soil and the Environment. SSSA, Madison, WI, pp. 275–294. https://doi.org/10.2136/sssaspecpub2162.2014.0044. SSSA Spec. Publ. 62.
Zhu, Y., Wu, F., He, Z., Giesy, J.P., Feng, W., Mu, Y., Feng, C., Zhao, X., Liao, H., Tang, Z., 2015b. Influence of natural organic matter on the bioavailability and preservation of organic phosphorus in lake sediments. Chem. Geol. 397, 51–60.
Zhu, Y., Wu, F., He, Z., Guo, J., Qu, X., Xie, F., Giesy, J.P., Liao, H., Guo, F., 2013b. Characterization of organic phosphorus in lake sediments by sequential fractionation and enzymatic hydrolysis. Environ. Sci. Technol. 47, 7679–7687.
Zhu, Y., Zhang, R., Wu, F., Qu, X., Xie, F., Fu, Z., 2013c. Phosphorus fractions and bioavailability in relation to particle size characteristics in sediments from Lake Hongfeng, Southwest China. Environ. Earth Sci. 68, 1041–1052.

Supplementary data

Manuscript title: Bioavailability and Preservation of Organic Phosphorus in Lake Sediments: Insights from Enzymatic Hydrolysis and ^{31}P Nuclear Magnetic Resonance

Authors: Yuanrong Zhu [a], Weiying Feng [a], Shasha Liu [a], Zhongqi He [b], *Xiaoli Zhao* [a, *], Yong Liu [c, d], Jianyang Guo [d], John P. Giesy [a, e], Fengchang Wu [a]

Index

Submitted to: *Chemosphere*

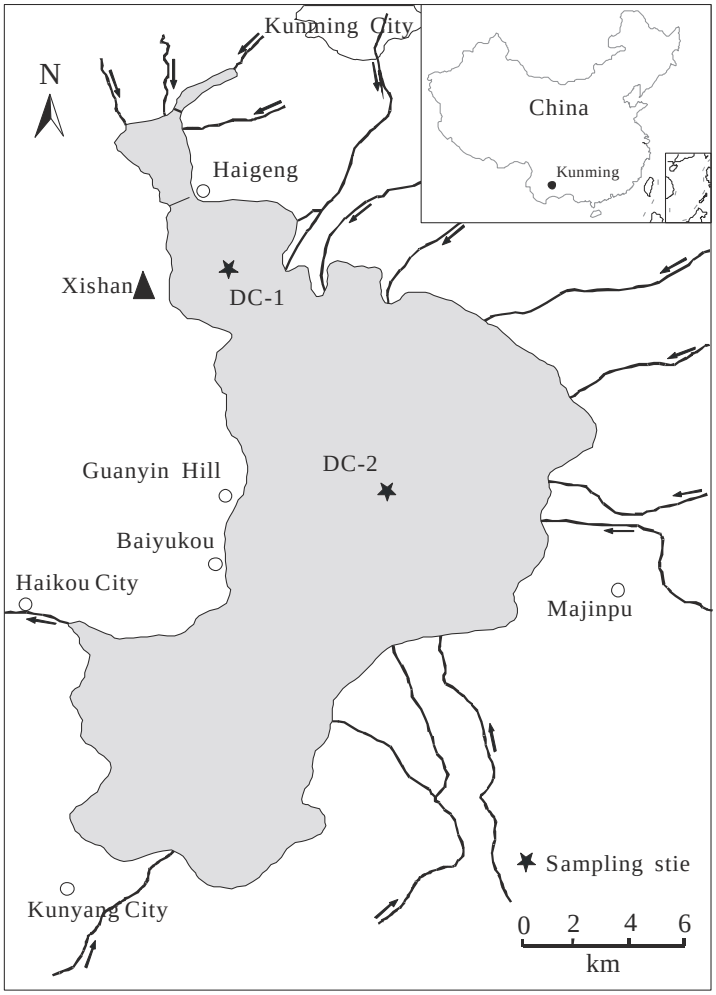

Figure S1 Map of Lake Dianchi showing coring sites (DC-1 and DC-2).

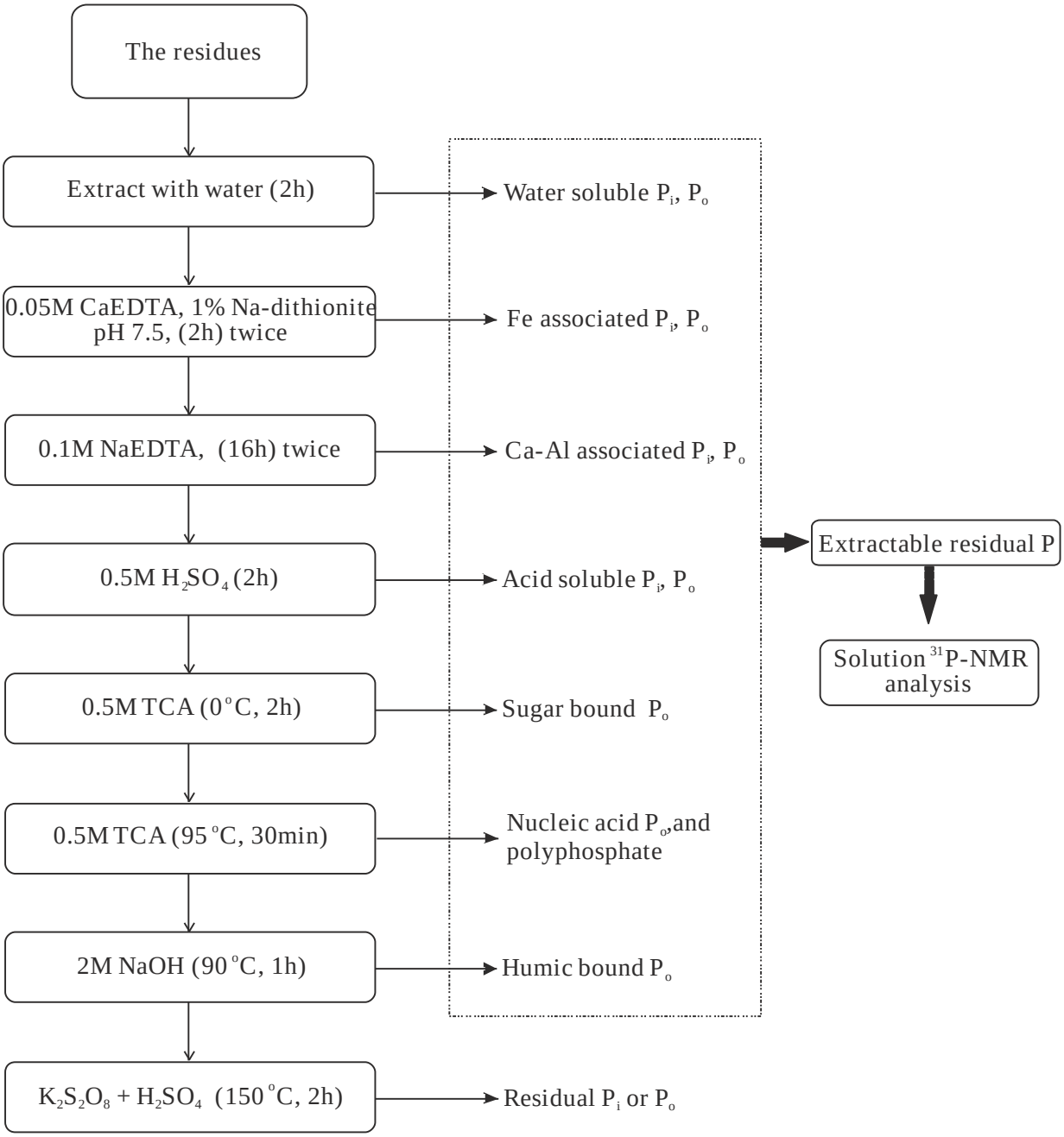

Figure S2. Sequential extraction procedure of organic phosphorus for residues after NaOH-EDTA extraction.

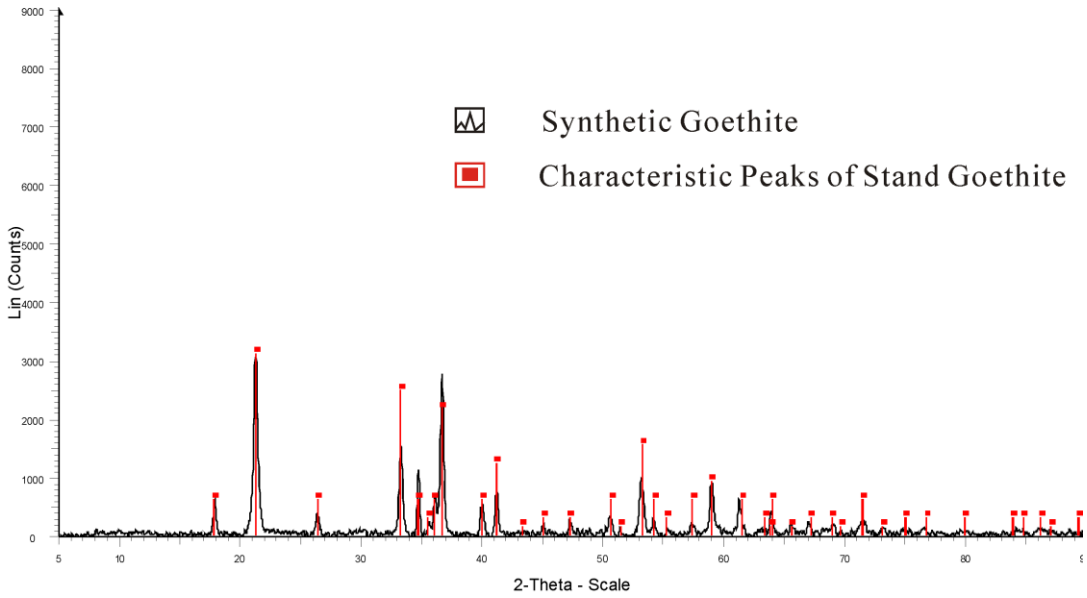

Figure S3. X-Ray Diffraction analysis of synthesized goethite.

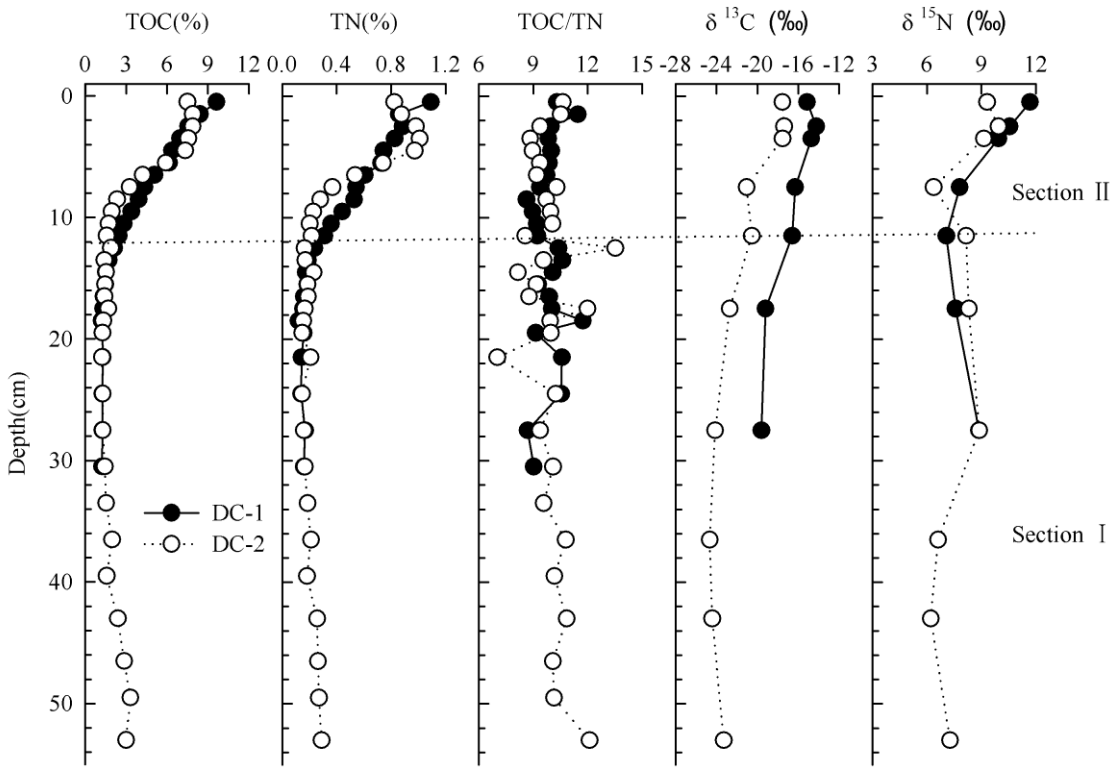

Figure S4. Vertical distributions of TOC, TN, TOC/TN (molar ratio), $\delta^{13}C$ and $\delta^{15}N$ in sediment profiles from DC-1 and DC-2.

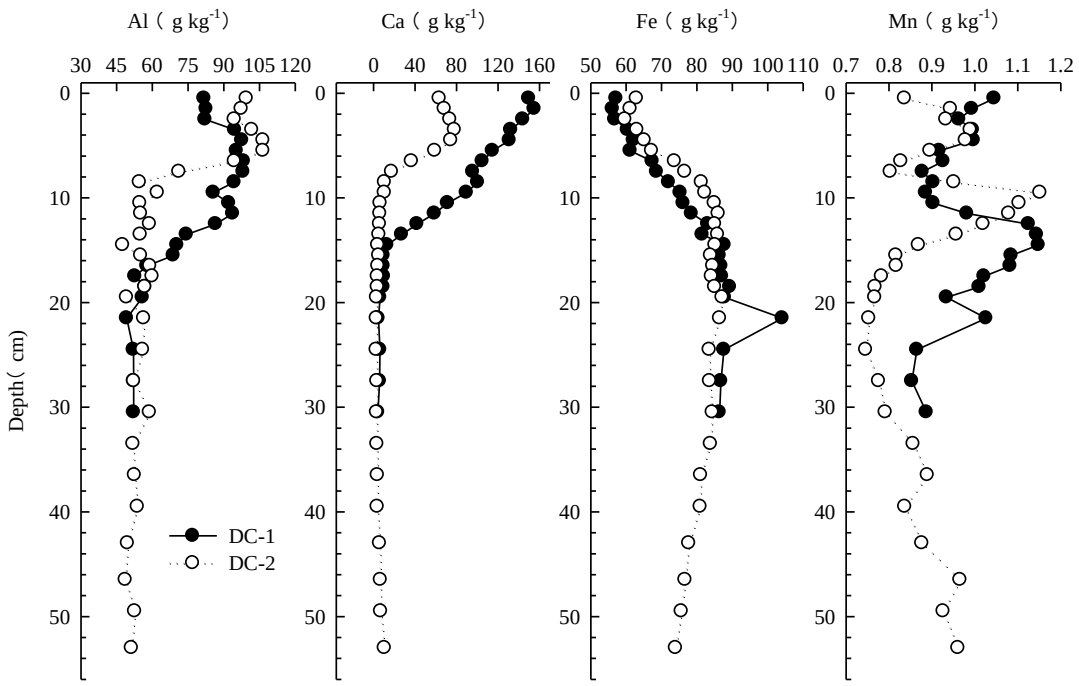

Figure S5. Distribution of Al, Ca, Fe, Mn contents in the sediment profiles (DC-1, DC-2).

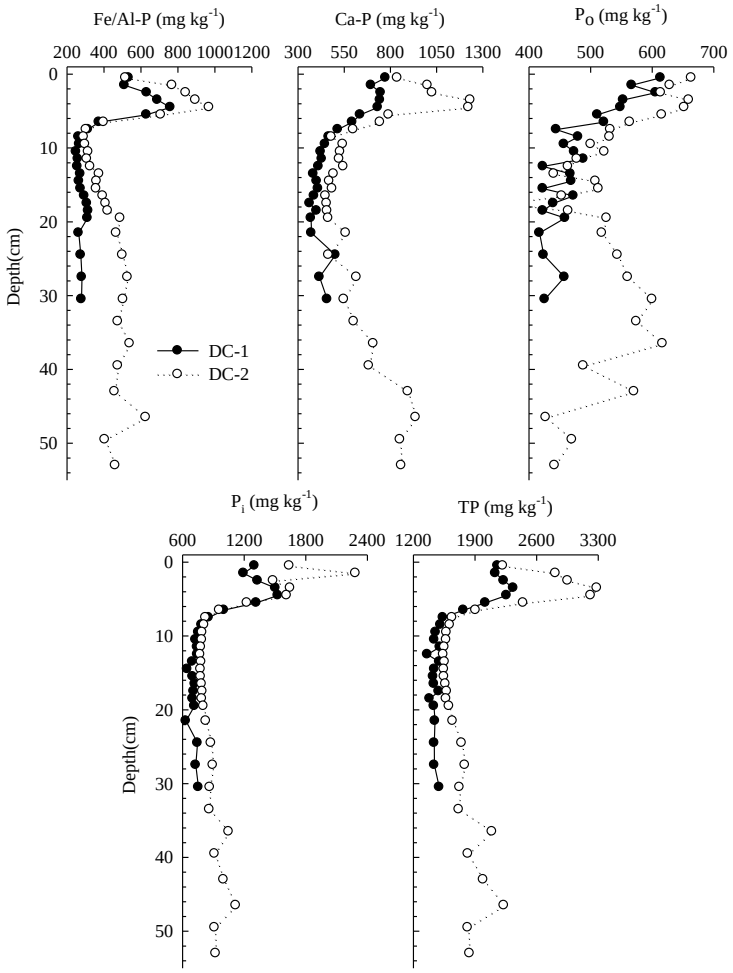

Figure S6. Vertical distributions of P fractions in sediment profiles from DC-1 and DC-2.

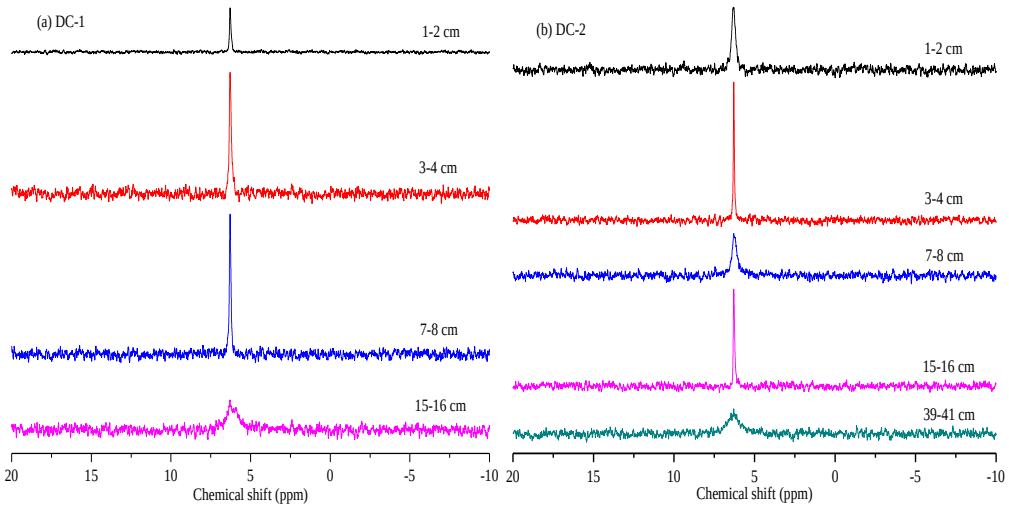

Figure S7. Solution ^{31}P NMR spectra for extractable residual P in the sediments (mixtures extracted by water, CaEDTA, NaEDTA, H_2SO_4 (neutralization by NaOH), cold TCA (0 ^{o}C), hot TCA(95 ^{o}C) and hot NaOH after NaOH-EDTA extraction).

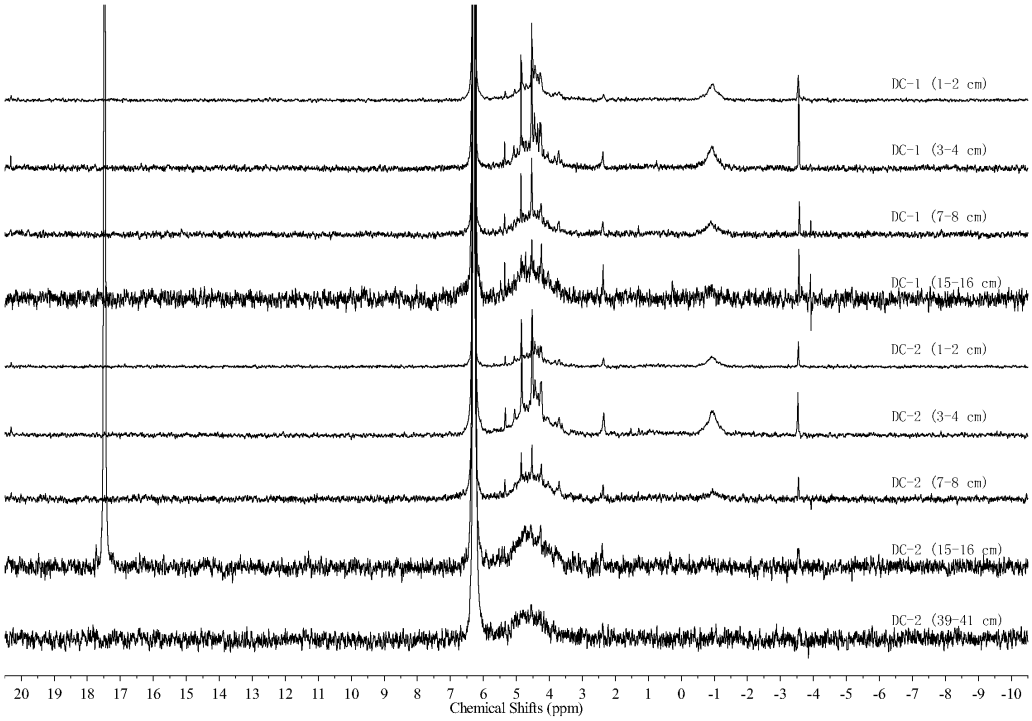

Figure S8. Solution ^{31}P NMR spectra for NaOH-EDTA extractable P_o in the sediments from Lake Dianchi. MDPA (methylene diphosphonic acid sodium salt) as an internal standard added to the sample of DC-2 (15-16 cm). Assignments of peaks are given in Figure 5.

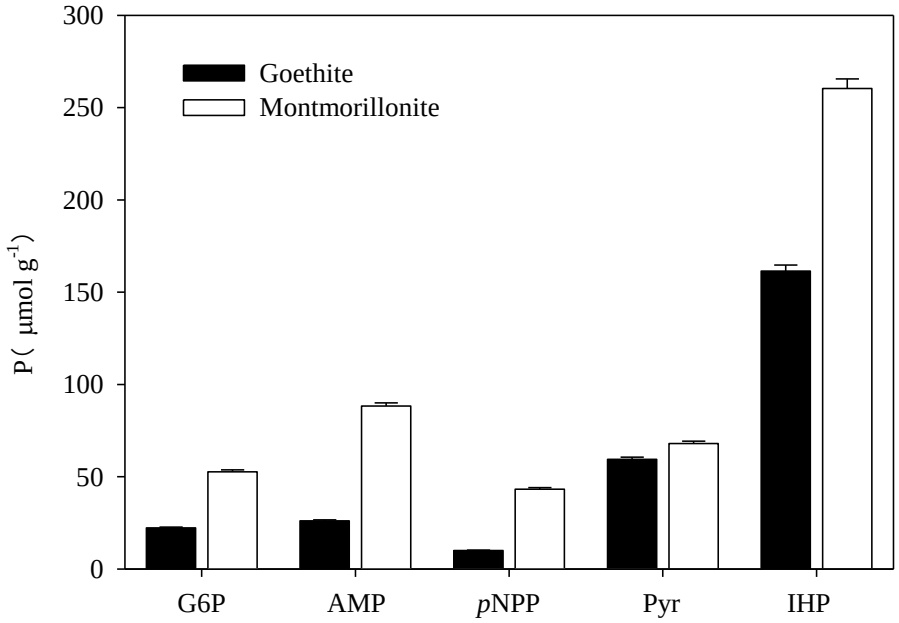

Figure S9. Concentrations of P_o and condensed P adsorbed by goethite or montmorillonite. Conditions: pH 9.0 for G6P, AMP, *p*NPP and Pry in Tri-HCl buffer; pH 5.15 for IHP in NaAc-HAc buffer. Keep the same conditions for the experiment of enzymatic hydrolysis.

Table S1. Percentage (%) of P_o extracted by NaOH-EDTA, and proportions (% of P_o hydrolyzed in NaOH-EDTA P_o) of NaOH-EDTA P_o hydrolyzed by enzymes in the sediment from DC-1.

Sediment Depth (cm)	NaOH-EDTA P_o /TP [a]	NaOH-EDTA P_o /SMT P_o [b]	APase (at pH 9.0, 37 ^oC) [c]	APase+PDEase (at pH 9.0, 37 ^oC) [c]	APase+PDEase+ Phytase (at pH 7.0, 37 ^oC) [c]
0-1	12.5	43.8	30.6	44.6	34.6
1-2	11.4	42.8	25.4	43.4	43.8
2-3	9.4	34.7	22.3	39.9	37.4
3-4	7.7	32.7	22.8	42.9	39.6
4-5	6.9	28.5	21.7	34.0	31.3
5-6	8.5	33.4	15.9	29.5	36.7
6-7	7.6	25.9	22.9	42.7	37.4
7-8	7.9	27.2	17.9	30.5	43.1
8-9	7.5	23.7	13.6	33.1	16.6
9-10	7.1	22.5	19.2	35.6	24.4
10-11	5.7	17.3	18.0	38.1	26.0
11-12	5.5	17.0	17.0	36.4	34.4
12-13	6.1	19.5	24.7	43.3	20.0
13-14	4.9	15.7	18.3	43.3	24.2
14-15	3.7	11.3	22.5	40.4	19.0
15-16	3.7	12.5	43.2	72.5	7.9
16-17	2.9	8.9	36.1	55.0	13.7
17-18	3.5	11.7	19.4	40.4	19.8
18-19	3.6	11.8	26.3	36.5	0.0
19-20	3.1	9.8	42.9	67.2	0.0
20-23	3.5	12.2	20.1	45.6	3.2
23-26	3.1	10.6	9.7	27.1	3.2
26-29	2.9	9.2	33.7	65.6	5.8
30-32	2.1	7.2	9.6	25.6	5.1

[a] Values are percentage (%) of NaOH-EDTA P_o in TP of sediments.

[b] Values are percentage (%) of P_o extracted by NaOH-EDTA in P_o determined by SMT protocol from sediments.

[c] Values are percentage (%) of P_o hydrolyzed by phosphatase in NAOH-EDTA P_o.

Table S2. Percentage (%) of P_o extracted by NaOH-EDTA, and proportions (% of P_o hydrolyzed in NaOH-EDTA P_o) of NaOH-EDTA P_o hydrolyzed by enzymes in the sediment from DC-2.

Sediment Depth (cm)	NaOH-EDTA P_o /TP [a]	NaOH-EDTA P_o /SMT P_o [b]	APase (at pH 9.0, 37 ^oC) [c]	APase+PDEase (at pH 9.0, 37 ^oC) [c]	APase+PDEase+ Phytase (at pH 7.0, 37 ^oC) [c]
0-1	9.3	31.1	48.6	60.0	40.7
1-2	7.5	33.6	42.5	55.7	42.1
2-3	7.5	35.8	38.9	48..4	37.4
3-4	5.7	28.5	36.9	43.5	38.4
4-5	6.3	30.9	36.4	42.5	32.1
5-6	7.4	29.5	36.8	45.3	36.7
6-7	6.7	22.7	36.6	48.7	40.3
7-8	6.7	20.8	27.2	36.1	53.1
8-9	5.5	16.9	35.9	40.6	59.1
9-10	5.3	16.6	27.2	43.7	55.3
10-11	3.3	10.0	62.8	97.4	68.2
11-12	4.6	15.1	51.8	83.4	67.5
12-13	3.8	12.6	50.9	81.7	74.2
13-14	3.6	12.6	66.9	100.0	76.4
14-15	3.8	11.6	37.0	59.8	58.4
15-16	3.0	8.9	73.3	100.0	84.9
16-17	4.0	13.7	38.8	52.1	83.9
17-18	1.9	8.4	54.6	100.0	87.3
18-19	3.4	11.6	39.0	73.7	68.9
19-20	3.7	11.2	53.4	61.4	54.3
20-23	2.4	7.8	35.3	82.5	73.9
23-26	1.9	6.1	67.6	100.0	57.4
26-29	3.4	10.7	20.6	56.0	69.5
30-32	2.6	7.4	31.3	65.2	80.5
32-35	2.4	7.1	49.9	100.5	34.4
36-38	1.6	5.4	56.3	84.0	85.1
39-41	2.2	8.2	26.0	76.0	31.2
41-45	1.8	6.3	47.3	49.2	100.0
45-48	1.9	10.0	15.1	48.7	81.2
48-51	2.5	9.6	25.1	58.2	86.4
52-55	2.5	10.3	28.9	34.1	66.6

[a] Values are percentage (%) of NaOH-EDTA P_o in TP of sediments.

[b] Values are percentage (%) of P_o extracted by NaOH-EDTA in P_o determined by SMT protocol from sediments.

[c] Values are percentage (%) of P_o hydrolyzed by phosphatase in NAOH-EDTA P_o.

Table S3. Mean contents of inorganic P (P_i) and organic P (P_o) forms (mg kg^{-1}) in sediment residues after extraction by NaOH-EDTA.

Sites	Depth	H_2O, P_i	H_2O, P_o	Ca-EDTA, P_i	Ca-EDTA, P_o	Na-EDTA, P_i	Na-EDTA, P_o	H_2SO_4, P_i	H_2SO_4, P_o	Cold TCA, P_i	Cold TCA, P_o	Hot TCA, P_i	Hot TCA, P_o	NaOH, P_i	NaOH, P_o	Residual P
DC-1	1-2cm	31.7	22.7	32.0	14.3	32.1	4.8	57.8	–	20.9	0.2	26.6	10.5	167.3	13.8	85.0
	3-4cm	31.4	15.8	24.0	– [a]	11.6	–	41.9	–	29.0	2.9	25.1	8.3	195.2	8.5	91.0
	7-8cm	33.2	0.4	27.3	1.9	18.0	0.5	26.9	–	23.3	4.8	18.1	9.7	203.5	9.0	101.8
	15-16cm	17.8	–	33.6	1.3	11.5	3.1	39.6	–	24.6	3.2	12.2	8.6	207.7	5.1	90.3
DC-2	1-2cm	36.1	13.6	19.3	12.4	21.1	–	78.3	–	26.1	1.3	33.3	13.2	214.2	19.2	102.7
	3-4cm	36.0	8.2	36.5	–	15.8	0.8	58.0	–	22.8	1.6	28.9	11.8	226.1	11.0	107.7
	7-8cm	19.0	–	23.1	4.3	18.4	–	41.3	–	26.4	2.8	20.6	9.3	219.5	16.2	114.3
	15-16cm	14.6	–	27.9	8.9	23.7	–	69.2	–	27.2	2.8	14.4	7.8	207.5	11.2	103.0
	39-41cm	16.5	–	32.6	–	25.3	–	25.1	–	25.7	1.4	17.5	8.6	252.2	–	89.4

"–" negative value, cannot be detectable

Table S4. Distribution (%) and recovery (%) of P in the mineral-P suspensions (APase buffer solution and enzyme free buffer) after incubation.

	Enzymatic hydrolysis					Buffer controls				
	Supernatants		NaOH extractable P		Recovery	Supernatants		NaOH extractable P		Recovery
	P_i	Condensed P or P_o	P_i	Condensed P or P_o		P_i	Condensed P or P_o	P_i	Condensed P or P_o	
G-G6P [a]	4.1	0	64.9	20.0	89.0	0.0	27.0	21.6	81.9	130.5
G-AMP	17.0	0	77.5	16.2	110.6	0.0	32.4	3.8	76.5	112.8
G-*p*NPP	0.0	0	118.3	0.0	118.3	0.0	9.4	86.1	18.7	114.2
G-Pyr	6.1	0	11.0	52.1	69.3	1.1	2.5	7.8	58.7	70.1
M-G6P [b]	27.8	0	69.0	15.9	112.6	0.0	33.7	40.2	39.8	113.7
M-AMP	38.8	0	44.3	11.6	94.8	0.0	27.2	18.7	30.3	76.2
M-*p*NPP	34.1	0	90.4	12.4	136.9	0.0	45.0	69.2	7.4	121.5
M-Pyr	19.9	0	35.6	23.8	79.3	3.3	3.4	34.6	64.2	105.6

[a] G, goethite; G-G6P, goethite-G6P complex

[b] M, montmorillonite

Table S5. Desorption (μmol g^{-1}) of inositol hexakisphosphate (IHP) from the mineral-IHP complexes in the NaAc-HAc buffer (enzyme free, buffer controls).

Incubation time/complex	G-IHP [a]		M-IHP [b]	
	TP	P_o	TP	P_o
2h	2.3	1.0	0.2	- [c]
6h	1.2	0.2	0.1	-

[a] G, goethite; G-IHP, goethite-inositol hexakisphosphate complex

[b] M, montmorillonite

[c] "-" not detectable